



sgem

Smart Grids and Energy Markets



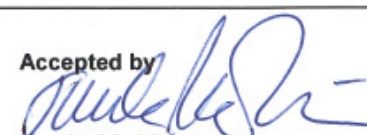
VTT-R-06033-14

AC/DC hybrid distribution system concept

Authors: Riku Pasonen

Confidentiality: Public



Report's title AC/DC hybrid distribution system concept	
Customer, contact person, address Cleen Ltd.	Order reference
Project name SGEM Smart Grids and Energy Markets	Project number/Short name 85060 - CLEEN/SGEM V 2014/ENE
Author(s) Riku Pasonen	Pages 35 (including 2 appendix pages)
Keywords LVDC, hybrid, microgrid, smart grid	Report identification code VTT-R- 06033-14
Summary	
<p>This paper studied the concept of hybrid AC/DC distribution with a shared neutral conductor. The main focus was on developing a concept and model around the idea of shared neutral conductor between AC and DC systems. A neutral conductor is unloaded when there is a symmetrical three-phase AC load. The idea was to find use of this capacity by injecting DC current into the neutral line. While power capacity was the focus in the actual simulations, microgrid operation and typical faults were also simulated. The results indicate that from a total system capacity perspective it is more favourable for this hybrid concept to have DC load than asymmetric AC load. By moving single-phase load to the DC side of the hybrid system, load could be increased from 10 kW to 19 kW (230 VDC simulation). DC load power could be increased by 12%, while symmetric AC load was increased by 67% when modelled with a star connection. With delta AC load, there was no change in DC system capacity with respect to symmetric AC power. Asymmetric AC load naturally limited the DC capacity due to shared wire. The study also carried out fault simulations concerning three-phase short circuits, short circuits in the DC system, and combined neutral breaking. A study was made of the model's fault current output when current limiting was programmed to an AC-side inverter and DC-side converter. Programmable fault current limiting worked better on the AC side than on the DC side in limiting the peak fault current, although steady-state current limiting worked well with both. Faults in the combined neutral conductor were naturally critical for operation.</p> <p>It can be concluded from the simulations that it is technologically possible to combine with an AC distribution system using a joint neutral and DC conductor. Power capacity increased by this method is, however, very limited (max 20% in this case) and varies according to the symmetrical load on the AC side. Of course, higher voltage would increase capacity, but would also require energy conversion at the client end. As this study has been carried out from a purely technological perspective, an economic analysis of possible scenarios would be needed to establish the competitiveness of the concept. Because capacity increases are quite modest, they cannot justify the use of this kind of concept. Possible use cases in mind were the increased reliability provided by the parallel DC system in providing backup power, and the DC system as the point where critical loads such as computers and lighting could be connected, as well as a simpler way of connecting small-scale generation. Using DC sockets would be an easy way to differentiate loads which will operational when the AC grid is down. LVDC is a good option from the reliability perspective, but should be built truly independently from the AC system, with no shared wire or "weak point".</p>	
Confidentiality	Public
Espoo 17.12.2014	
Written by  Riku Pasonen Research Scientist	Reviewed by  Marja-Leena Pykälä Senior Scientist
Accepted by  Tuula Mäkinen Head of Research Area	
VTT's contact address Riku Pasonen, riku.pasonen@vtt.fi, PL 1000, 02044 VTT	
Distribution (customer and VTT) CLEEN, SGEM	
<p><i>The use of the name of the VTT Technical Research Centre of Finland (VTT) in advertising or publication in part of this report is only permissible with written authorisation from the VTT Technical Research Centre of Finland.</i></p>	

Preface

This work was carried out in the Smart Grids and Energy Markets (SGEM) research programme, coordinated by CLEEN Ltd, with funding from the Finnish Funding Agency for Technology and Innovation, Tekes. The purpose of this work is to investigate a hybrid AC/DC distribution system concept.

Contents

Preface.....	2
Contents.....	4
1. Introduction.....	5
2. Hybrid LV distribution system concept	5
2.1 Technical requirements and limitations	5
2.2 Operational modes	6
3. Simulation model	8
3.1 Simulation model main components	8
3.1.1 Grid connection model	8
3.1.2 Inverter	9
3.1.3 Synchronization system	11
3.1.4 DC/DC converter.....	12
3.1.5 Energy storage	13
3.1.6 PV production	14
3.1.7 Loads and distribution line	15
4. Simulation cases.....	15
4.1 System functionality test simulation	15
4.2 Simulations to study power capacity limits	17
4.2.1 AC system only.....	17
4.2.2 Hybrid system with symmetric AC load	18
4.2.3 Hybrid system with 5% voltage rise on neutral	19
4.2.4 Hybrid system with AC unbalance.....	20
4.3 DC voltage adjusted to peak value of AC voltage	21
4.3.1 Hybrid system, 90 kW symmetric AC, 5% voltage rise on neutral	21
4.3.2 Hybrid system, 90 kW symmetric +10 kW single phase AC, 5% voltage rise on neutral.....	22
4.3.3 Hybrid system maximum power with 325 V DC voltage	23
4.4 Fault simulations.....	23
4.4.1 Over-current protection AC part of the concept	23
4.4.2 Over-current protection DC system	26
4.4.3 Overvoltage protection.....	27
4.4.4 Combined neutral conductor fault simulations.....	28
5. Results.....	31
6. Conclusions	32
References.....	32

1. Introduction

At the end of 19th century, alternating current (AC) and direct current (DC) systems were fighting for the position of dominant electric transmission system. AC systems won the battle then, but the importance of DC electricity has increased in energy production with the rise of photovoltaic panels which output DC. DC transmission is also used today in long-distance high-voltage cables, such as transmission cables on the floors of oceans.

The integration of renewable energy production and energy storages into power grids is a common research topic. What makes this demanding is that most of PV production is installed in an LV distribution system. One option for making this easier is to change LV distribution to DC and convert the voltage to AC at the customer premises. This publication investigates a further option, namely a concept for integrating a low voltage direct current system (LVDC) into current LVAC distribution systems to form a hybrid transmission system. The concept presented here also enables microgrid operation. Microgrids are electric power systems that can operate independently from main distribution systems by having their own production units and power quality control devices.

2. Hybrid LV distribution system concept

The defining factor of the AC/DC hybrid distribution concept presented here is use of the neutral wire to transmit DC current along with the asymmetric component of three-phase AC current. The result is a system with one less wire compared to two separate AC and DC systems. This will naturally increase the load on the neutral wire, so DC injection to the neutral conductor must be limited when the AC system requires more of the capacity. Figure 2.1 represents the general concept of the hybrid AC/DC distribution system.

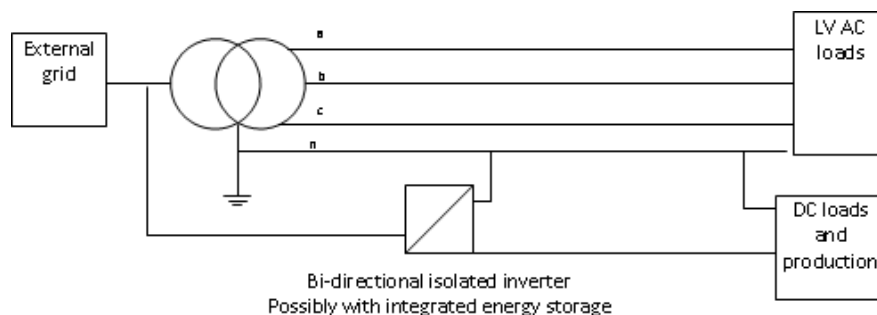


Figure 2.1. Hybrid AC/DC distribution system concept. Based on the figure presented in [1].

2.1 Technical requirements and limitations

To enable use of the neutral wire for the combined DC and asymmetric component of AC current, the converter in question must have galvanic isolation on the DC side so that simultaneous operation of the DC and AC system is possible in the manner presented in Figure 2.1. Without galvanic isolation, the converter would create a short circuit. Control of the converter must be capable of operation in island mode if uninterruptable power supply is needed for the AC or DC side. DC should be able to operate independently if there is a fault in the AC system and vice versa. DC power capacity is clearly limited and variable, with the room available in the neutral conductor for DC current dependent on the status of the AC system. Although dimensioning of the neutral conductor sets the limit for maximum available DC power in a symmetric AC load situation, capacity is also affected by the 3rd harmonic. Figure 2.2 displays maximum current in a neutral conductor with respect to the 3rd harmonic in the phase conductor.

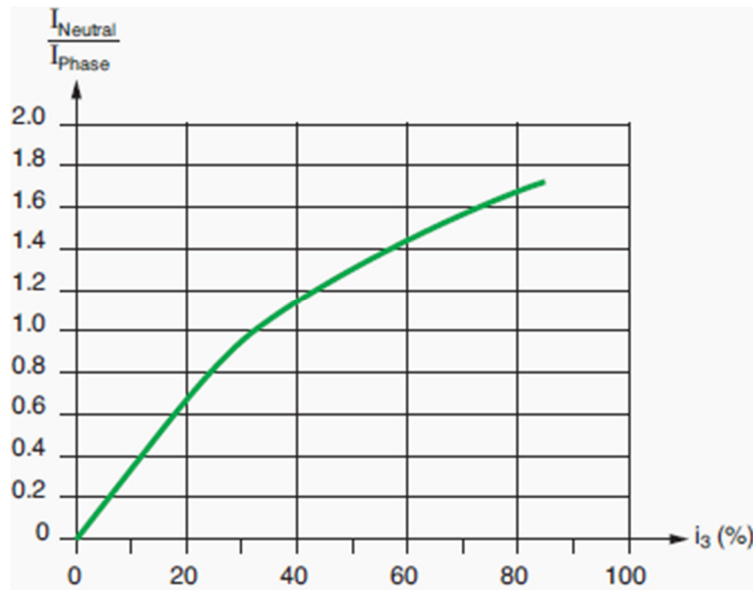


Figure 2.2. Maximum current in the neutral conductor with respect to 3rd harmonic percentage in a three-phase AC system. [2]

It can be seen from the figure that the 3rd harmonic greatly affects the neutral current, and would also take capacity from the DC current in the examined concept.

2.2 Operational modes

One of the main targets of the hybrid distribution concept is to achieve a system capable of operating in many different situations with respect to fault location. The following figures represent these modes. The green shapes represent parts that are functioning, and the red shapes the parts that are faulty or disconnected because of a fault. Figure 2.3 displays the system in normal operation.

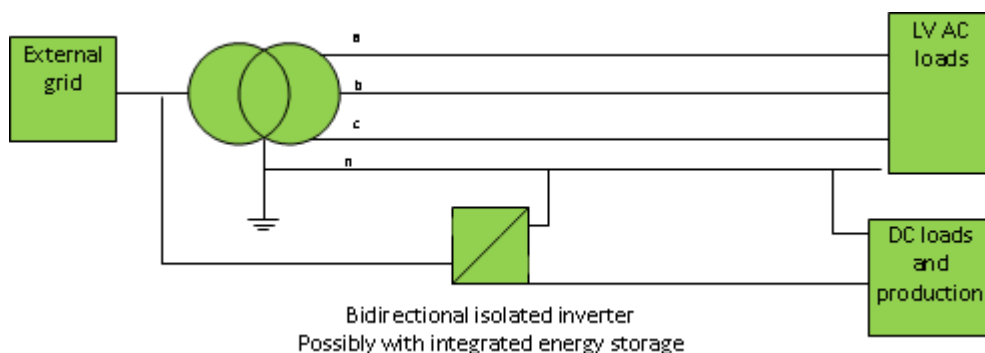


Figure 2.3. Parallel operation with AC grid. "Normal operation mode"

In normal operation mode, both systems operate in parallel. Control modes depend on how the system is to be used. On a general level, the inverter operates in power control mode, and the DC side in voltage control mode. Figure 2.4 displays the system with external faults.

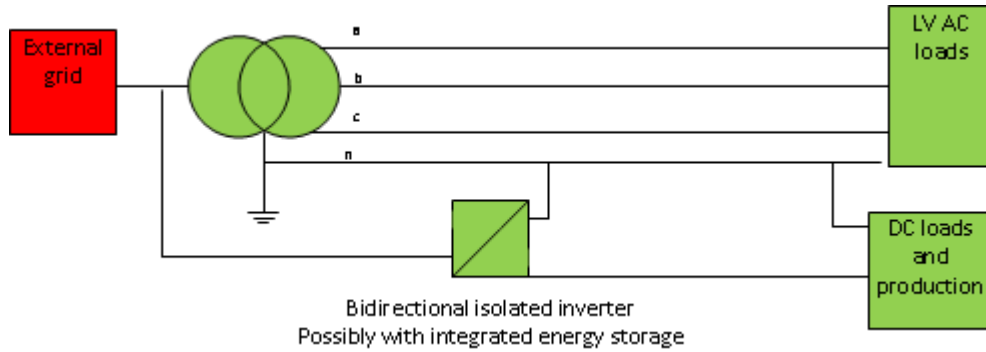


Figure 2.4. Failure in the external grid connection. "AC/DC microgrid operation"

The system should be able to continue to operate for some period after a fault occurs in the external grid. This can be described as AC/DC microgrid operation. Figure 2.5 displays the system with AC distribution faults.

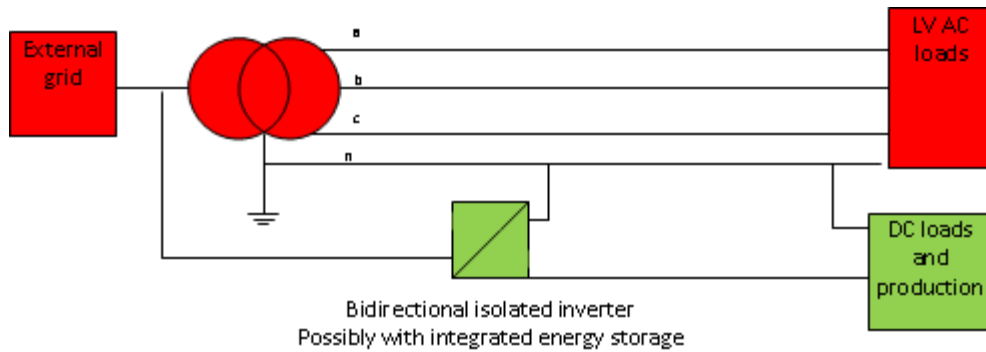


Figure 2.5. Failure of the entire AC system. "DC microgrid operation"

The whole AC system could be faulted, the DC part then operating as a microgrid (assuming the fault not to be in the neutral part of the AC system). Figure 2.6 displays the system with DC system faults.

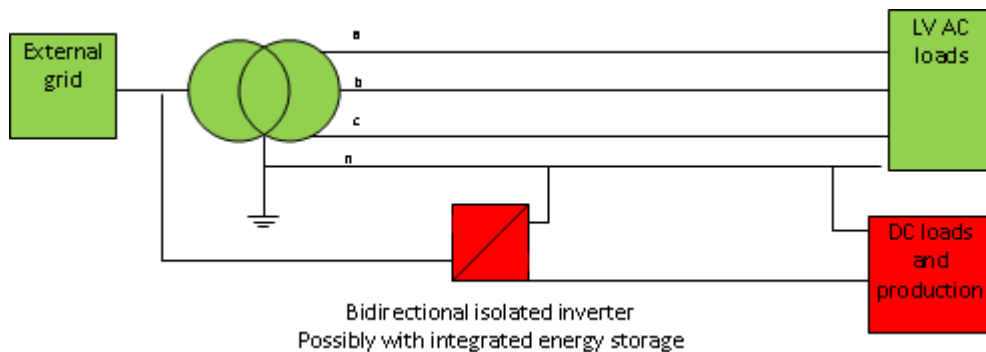


Figure 2.6. Failure in the DC system. "AC system operational"

Similarly, faults on the DC side should not affect operation of the AC system, and the DC system should be capable of shutting down safely in a fault situation.

3. Simulation model

The simulation model built for the task was made using a PSCAD transient simulator, developed by the Manitoba HVDC Research Centre. PSCAD can be used in transient simulation studies for accurate calculation of instantaneous values of currents and voltages in AC and DC systems. Version X4 of the program was used in this model.

3.1 Simulation model main components

The upper layer of the simulation model is presented in Figure 3.1.

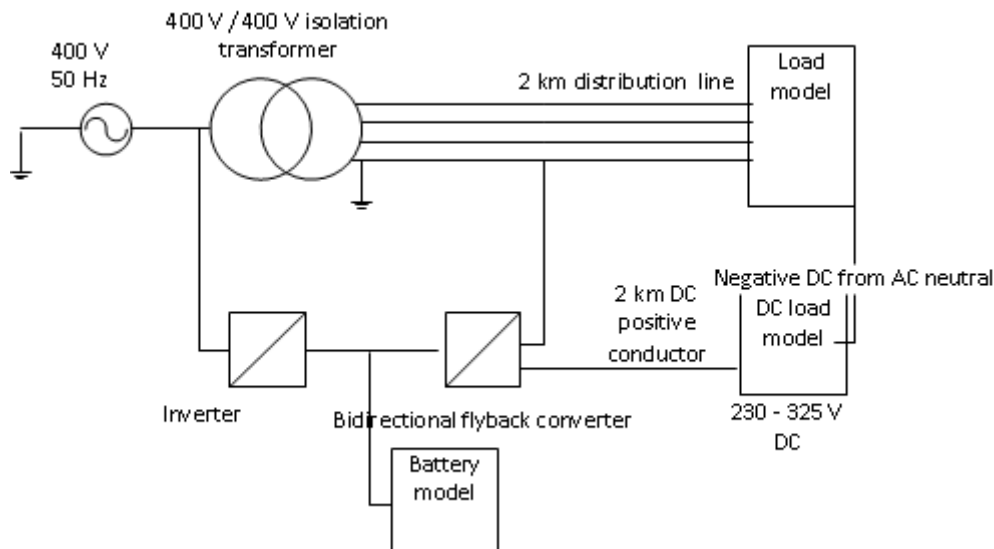


Figure 3.1. Principle representation of the upper layer of the simulation model

A detailed screen capture of the model in PSCAD is displayed in Appendix A. Individual parts of the model are described in detail in the following chapters.

3.1.1 Grid connection model

The grid connection is modelled with the ideal connection to the system. The choice of ideal connection (only 0.002 ohm resistance) is because of the need only to investigate voltage deviations caused by the LV system. Figure 3.2 displays the grid connection in the model.

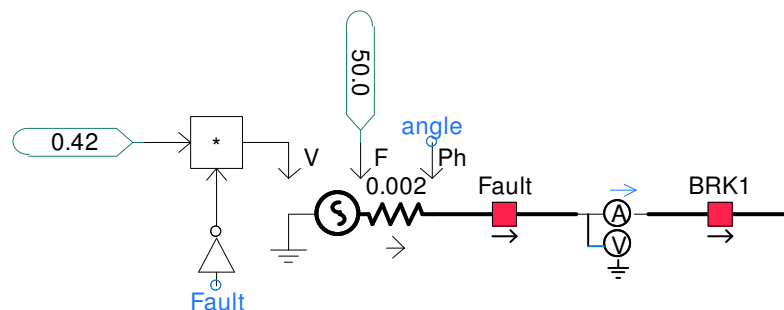


Figure 3.2. Grid connection model

In addition to the normal voltage source model, one breaker is added to act as a fault and another breaker to act as a protection device for the line. Voltage is also driven to zero during the fault. This is because opening the breaker does not actually remove the connection but inserts large resistance into the line. This could affect simulation accuracy when the breaker is open and the phase angle is measured close to the breaker.

3.1.2 Inverter

The inverter is needed for converting the DC current to AC. The inverter is configured to operate in power control mode when the AC grid has no fault, and in voltage control when supplying an isolated microgrid. Figure 3.3 displays the outer layer of the inverter simulation block and signal inputs and outputs.

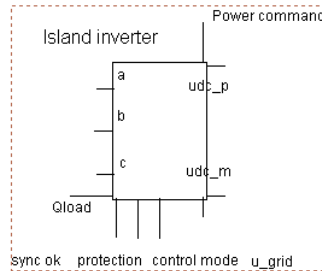


Figure 3.3. Inverter simulation block outer layer and external connection point

In addition to voltage connection points, there is output for phase difference stats (sync ok), protection relay status (protection), input for control mode selection and external input for voltage measurement from the grid side of the synchronisation relay. Figure 3.4 displays the circuit diagram of the inverter bridge and LCL filter.

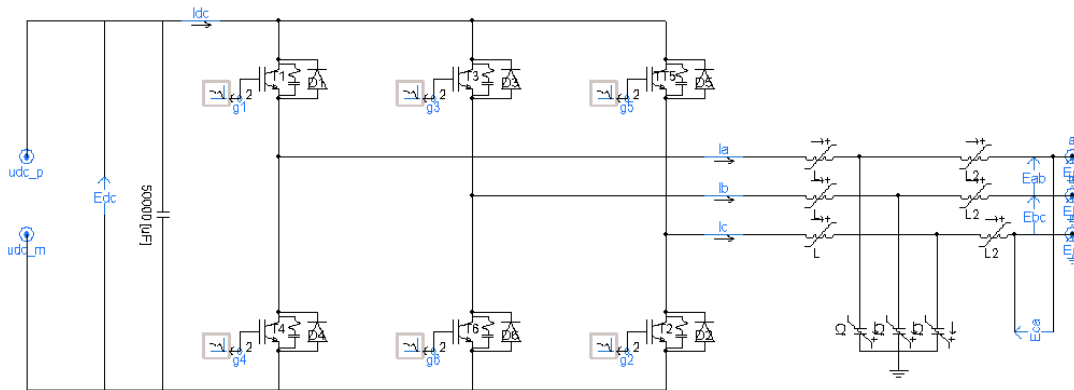


Figure 3.4. Circuit diagram of the inverter bridge and LCL filter.

The basic configuration of the inverter is based on that presented in [3]. The inverter control system has separate controls for grid connected operation and microgrid island operation. Figure 3.5 presents the control logic when in grid connected mode.

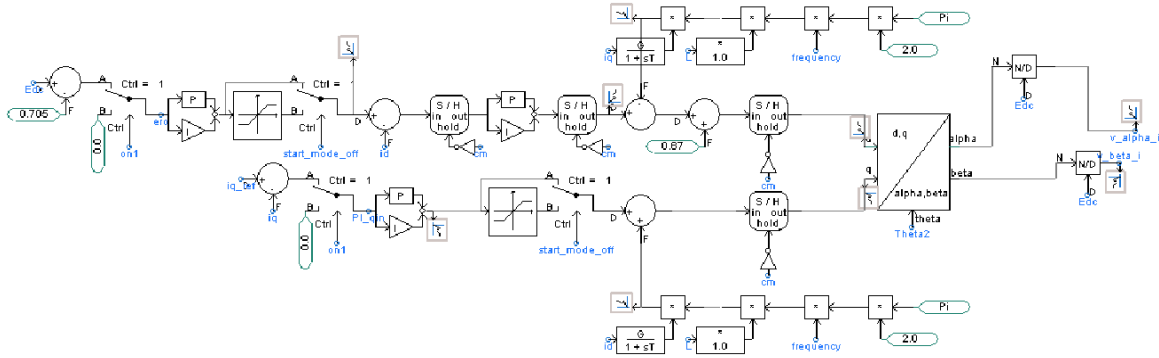


Figure 3.5. Inverter control for grid connected mode. A larger figure is presented in Appendix B.

In grid connected mode, the inverter is controlled so that voltage between the inverter and the DC/DC converter remains constant. This also keeps the battery state of charge (SOC) at an approximate constant. In a more sophisticated control method this mode could be adjusted to give direct control of the SOC. Figure 3.6 displays the inverter control logic in an islanded microgrid.

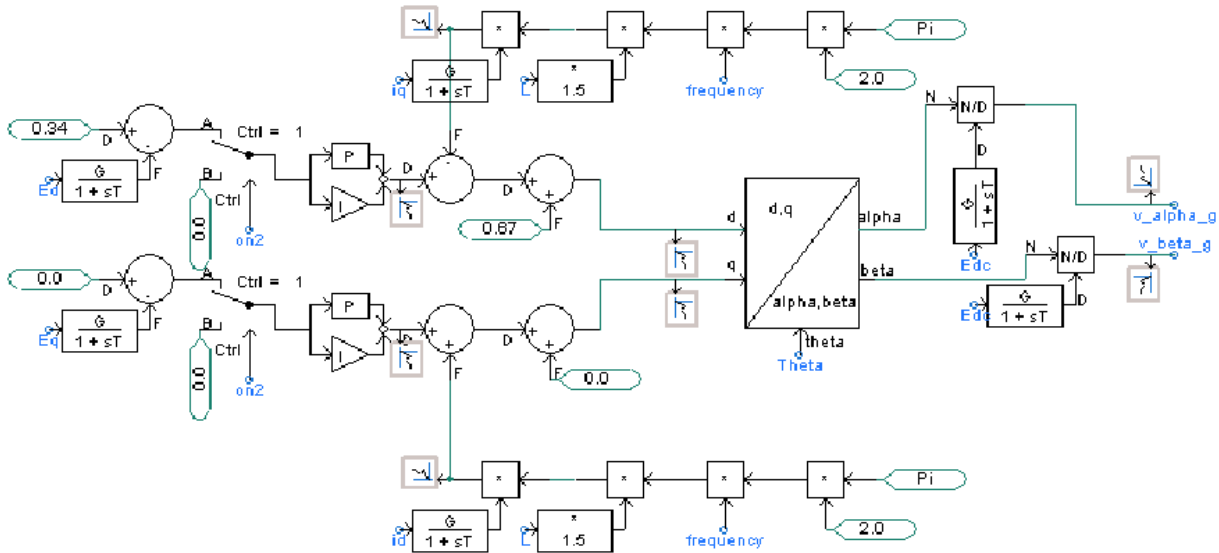


Figure 3.6. Inverter control logic in a microgrid

As mentioned previously, the inverter operates in voltage control mode when feeding the AC system during faulted supply from the upstream grid. The logic was created to control voltage with two PI controllers. This type of control can also be called single-loop control [4]. Voltage is measured and converted to a DQ system. Equation 1 displays the method of conversion of instantaneous values of phase voltages.

Equation 1. Conversion of phase voltages to a DQ system [5]

$$\begin{bmatrix} U_D \\ U_Q \\ U_0 \end{bmatrix} = \frac{2}{3} \begin{bmatrix} \cos(\phi) & \cos(\phi - \frac{2\pi}{3}) & \cos(\phi - \frac{4\pi}{3}) \\ -\sin(\phi) & -\sin(\phi - \frac{2\pi}{3}) & -\sin(\phi - \frac{4\pi}{3}) \\ \frac{1}{2} & \frac{1}{2} & \frac{1}{2} \end{bmatrix} \begin{bmatrix} U_a \\ U_b \\ U_c \end{bmatrix}$$

The phase angle in the transformation matrix is locked to phase “a” of the grid. PI controllers in both control systems are driven to zero when not used. Output signals would wander too far from the right setting if the unused control system remained active when switching to alternative control. In practice this would introduce current spikes when switching the control logic. Current references in the DQ system for power control can be calculated using the following equations.

Equation 2. Calculation of current reference using DQ voltages for active power (P)

$$id_ref = \frac{2 \cdot P}{3 \cdot Ud}$$

Equation 3 Calculation of current reference using DQ voltages for reactive power (Q)

$$iq_ref = \frac{2 \cdot Q}{3 \cdot Ud}$$

3.1.3 Synchronisation system

There are basically two ways of synchronising the generator to the AC system. Traditionally, the power generator frequency is driven close to the grid frequency, but with a deliberate small difference retained. This ensures that phase angles of the grid and device cross at some point in time. At this exact moment, the synchronisation relay closes and the generator is connected to the grid. The frequency difference nevertheless causes a short power spike when the generator is forced to accelerate or slow down to the grid frequency. Another option is to lock the frequency of the converter to the grid frequency, and adjust the phase angle to match the grid phase angle exactly. In theory, this method would not produce a power spike at synchronisation. The latter option is used in this model. Figure 3.7 displays the main part of the implementation of synchronisation in the model.

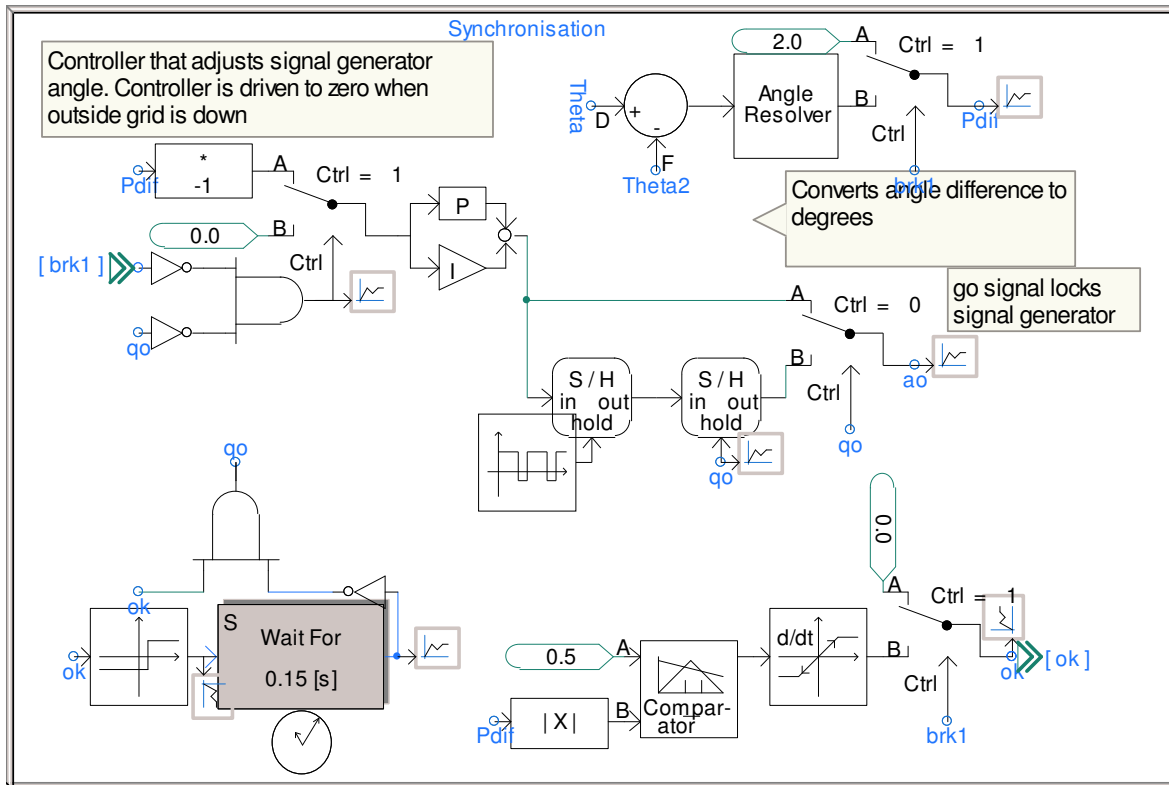


Figure 3.7. Main part of the model's synchronisation system

The synchronisation system measures an angle difference and converts it to degrees for the PI controller. The controller adjusts the phase angle of the signal generator used for making the reference signal for the inverter. Phase angle control is locked when the system operates as an island and the external grid is down.

3.1.4 DC/DC converter

The DC/DC converter in the concept is in charge of keeping DC voltage constant in the DC distribution line. Figure 3.8 displays the symbol for the converter module in the model.

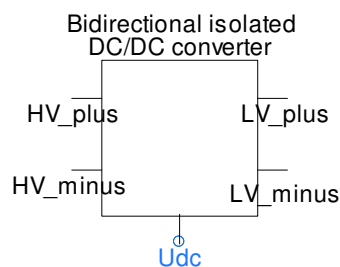


Figure 3.8. Bidirectional DC/DC converter with galvanic isolation

The converter layout is that of a bidirectional flyback converter. Galvanic isolation is achieved using transformer coils inside the converter. The converter design was presented in [1]. Figure 3.9 displays the principle circuit diagram of the converter.

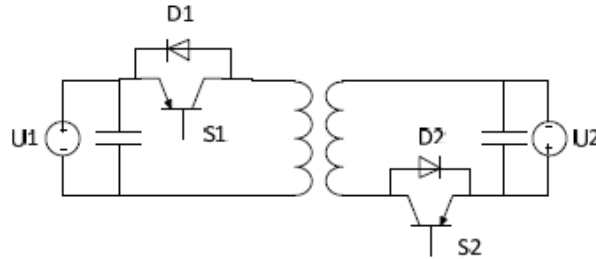


Figure 3.9. Principle circuit layout of the converter [1]

The converter is controlled in voltage control so that it keeps voltage constant at the DC bus. The converter control has individual controls for both power directions. Figure 3.10 illustrates the model's control logic implementation.

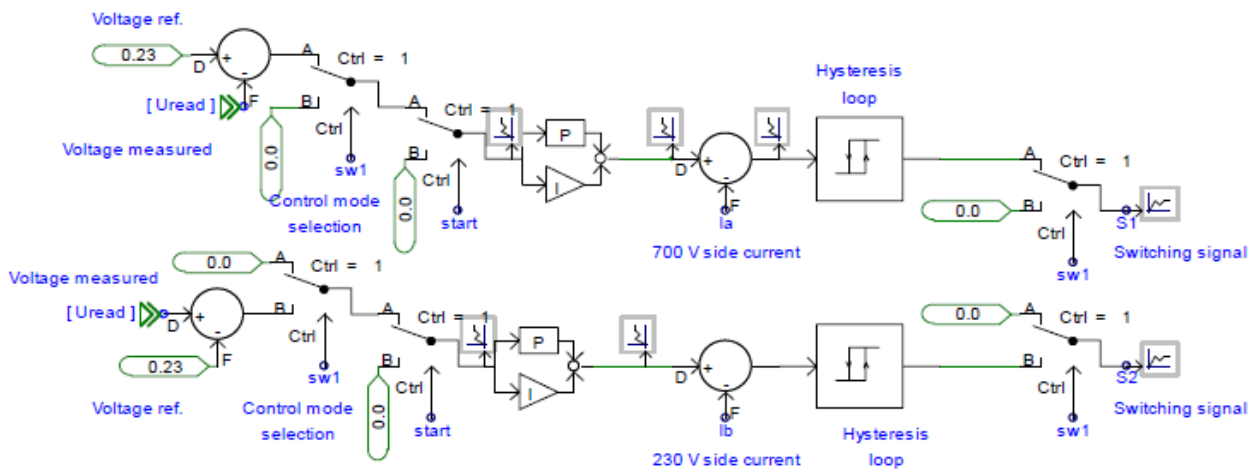


Figure 3.10. Control logic of the DC/DC converter [1]

The control operates by measuring voltage error and generating a current reference with the PI controller. The current reference is compared to the measured current, and the difference fed to a hysteresis generator which controls the actual power electronic switches. The control mode is selected by measuring which way voltage error occurs. This selection is presented in Figure 3.11.

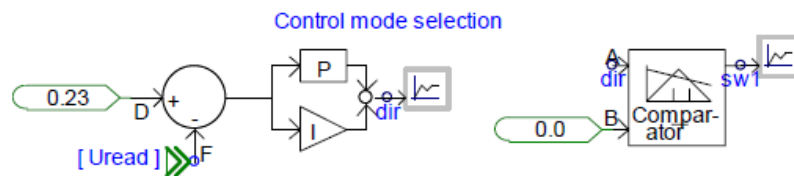


Figure 3.11. Control mode selection

The actual selection is made with a PI controller which improved the stability of the control mode selection signal.

3.1.5 Energy storage

A lead acid battery was chosen as energy storage for this model. The model is based on the CIEMAT model which was used in simulations in [6]. The model has different output voltage equations for discharge, charge, and overcharge situations. The reference product for the model is STECO Saphir 3600, the parameters of which have also been validated in [6]. An in-depth description of the battery component model can be found in [3].

3.1.6 PV production

PV production is modelled to be connected to a DC bus. The PV panel model is based on what was presented in [7]. The model was made with a single equation and current source. Equation 4 displays the equation.

Equation 4

$$I(V) = \frac{E_i}{E_{iN}} \cdot \frac{I_{sc}}{1 - \exp\left(\frac{-1}{b}\right)} \cdot \left(1 + \frac{TCi}{100} \cdot (T - T_N)\right) \cdot \left[1 - \exp\left(\frac{V}{b \cdot \left(\frac{V_{min}}{V_{oc}} + \left(1 - \frac{V_{min}}{V_{oc}}\right) \cdot \frac{E_i}{E_{iN}}\right) \cdot (V_{oc} + TCV \cdot (T - T_N))} - \frac{1}{b}\right)\right]$$

V	voltage of operation for the solar panel.	I_{sc}	short-circuit current under STC.
I	total output current for the solar panel.	V_{oc}	open circuit voltage under STC.
P	the solar panel total output power. ($P = V \cdot I$).	TCi	Temperature coefficient of I_{sc} .
R	internal resistance of operation. ($R = V/I$).	TCV	Temperature coefficient of V_{oc} .
T	solar panel temperature ($T_N = 25$ °C).	V_{min}	is the maximum voltage, when the irradiation level is less than 20% using the experimental I-V characteristic curve.
E_i	effective irradiance over the PVM ($E_{iN} = 1000$ W/m ²).	γ	is the shading linear factor for the V_{oc} .
b	I-V characteristic constant for the solar panel.		

To simplify the equation the following renaming can be used,

Equation 5

$$I(V) = a \left[1 - \exp\left(\frac{V}{b \times c} - \frac{1}{b}\right)\right]$$

This can be modified to operate as a voltage source type by solving voltage (V) with respect to current (I)

Equation 6

$$V(I) = c \left[\ln \frac{I}{-a} + \frac{1}{b}\right]$$

This voltage source version is used in the model. To model a large array of panels, V_{oc} , V_{min} and I_{sc} were multiplied to reflect configuration of multiple panels in series and in parallel. Figure 3.12 displays the PV module simulation block in the PSCAD program.

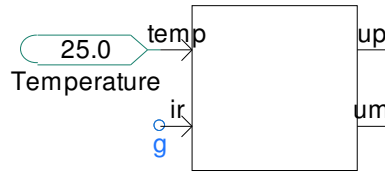


Figure 3.12. PV panel simulation block

Input signals for the block are solar radiation (ir) and temperature of the panel (temp). The PV module block was used in the model to test bidirectional capability of the DC/DC converter.

3.1.7 Loads and distribution line

Loads are modelled with three- and single-phase load models found from the PSCAD main library. In practice, three-phase load is star-connected impedance. The value of impedance is calculated from the nominal voltage value and from the given power set point of the user. Single-phase load is similar, but impedance is connected between one phase and neutral. The distribution line is modelled as two 185 mm² aluminium conductors in parallel. The length is set to 2 km. Lines are modelled with standard single-phase coupled PI sections found in the PSCAD main library. Table 1 has a list of the parameters used for the line model.

Table 1. Parameters for the AC line model (calculated for two Al 185 parallel lines from [8])

Phase resistance	8.85e-5 [ohm/m]
Phase reactance	2.670e-5 [ohm/m]
Susceptance	3.75e-4 [μ S/m]

The neutral line is assumed to have the same parameters as the phase conductors. Due to the inverter, the AC system also has a 200 kVA isolation transformer to create a true neutral for the system.

4. Simulation cases

Simulation cases are for the most part performed as comparisons with and without a hybrid distribution system. In addition to these studies, one simulation is carried out to verify the desired operation in an AC grid fault.

4.1 System functionality test simulation

In this test, the system is first started and normal operation continued parallel with the external grid. A fault in the AC system will occur at 0.6s of simulation time, after which the system is separated from the faulty external AC grid. At the same time as the system is switched to islanded operation mode, the control mode is changed to voltage control of the AC side of the distribution system. The fault is cleared from the external grid at 1.5 s of simulation time. The system then adjusts the voltage angle to match the grid. When voltage angle and frequency are equal, the system is again synchronised to the external AC grid. The load on the AC side is set as symmetric 100 kW. The DC system has only a PV panel producing 1.6 kW of power. Figure 4.1 displays the three-phase AC voltages in per unit values (1.0 equates to 400 VAC).

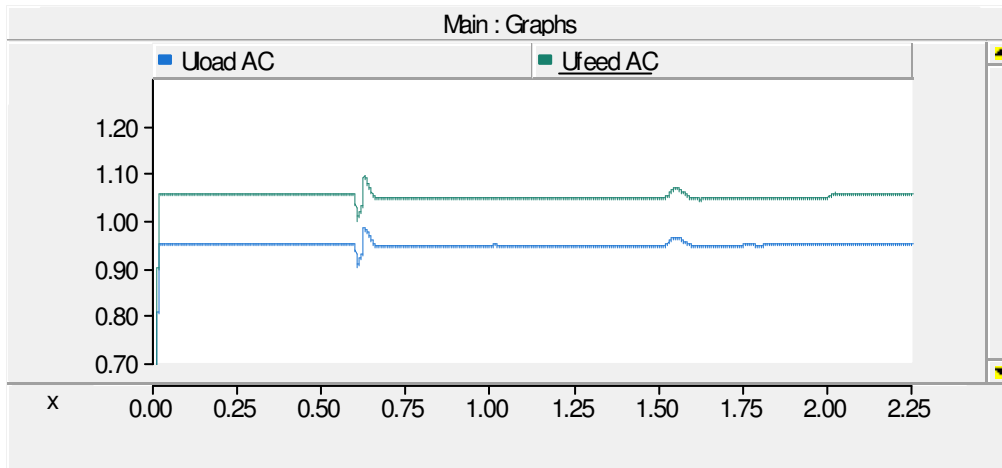


Figure 4.1. Measured voltages at the start (green) and end (blue) of the distribution line in per unit values with nominal voltage (1.0) of 400 V.

The first dip and spike in the figure is the point in time when the fault occurs in the AC supply and the system is switched to operate as an island. The second spike at 1.5 s occurs when the voltage angle is adjusted to match the external grid when the fault is cleared. At 2.0 s the system is again synchronised to the external grid. The voltage spike due to angle adjustment can be minimised with slower control. Here the simulation period is quite short, and control is fast. A closer look at the voltage after the 400 V/400 V isolation transformer during the fault and islanding is presented in Figure 4.2.

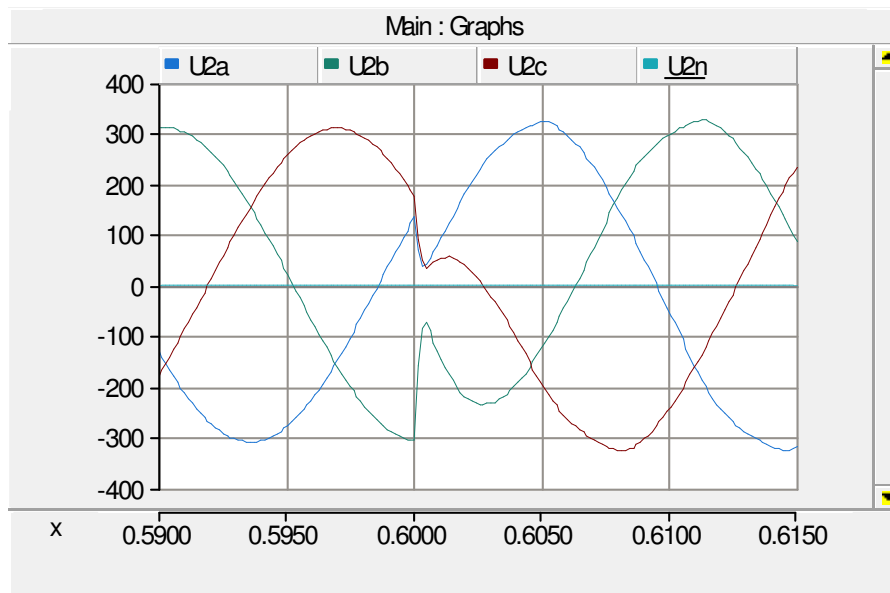


Figure 4.2. Shape of the voltage (V) when the operation mode is changed

The transformer smooths the noise from the voltage produced by the inverter. The voltage sag length depends on how fast the loss-of-mains protection can work. Here it would be ideal to view the performance of the converter control. The power output of the inverter is presented in Figure 4.3.

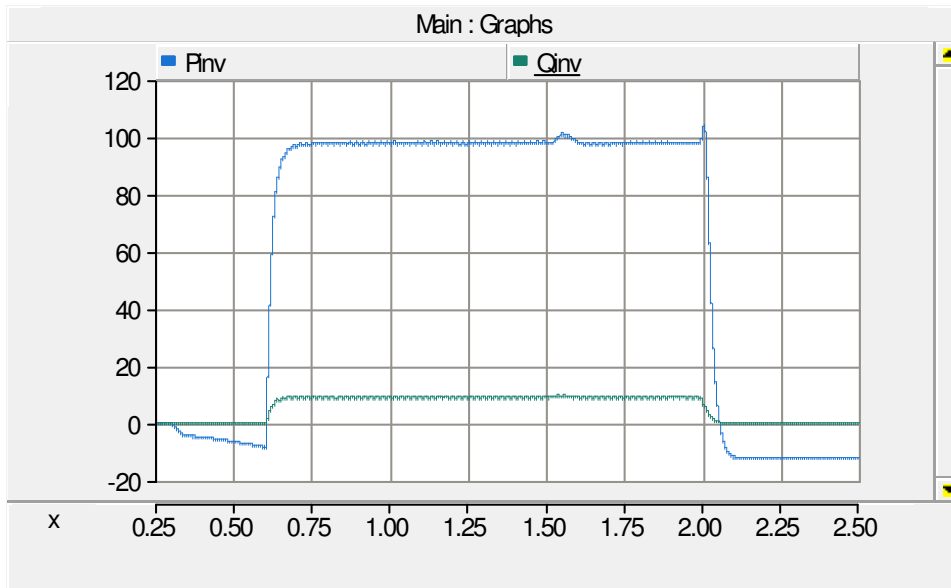


Figure 4.3. Power output of the inverter. Active power, kW (blue), reactive power, kVAr (green)

The inverter is charging the battery before the AC fault. The inverter starts feeding the AC load once the system is in island operation mode. There is a small change in power when the voltage angle is adjusted to match the grid at 1.5 s (see same spot in Figure 4.1).

4.2 Simulations for studying power capacity limits

In this chapter of simulations the AC load is varied from symmetric to asymmetric, and results with and without hybrid distribution are compared.

4.2.1 AC system only

Here symmetric AC load is set to 90 kW and single-phase load increased in one phase until voltage sag in that phase is 10% of nominal voltage. 10 kW seems to be a limit for the unbalanced load in this case. Figure 4.4 displays the corresponding phase voltages, measured at the load connection point.

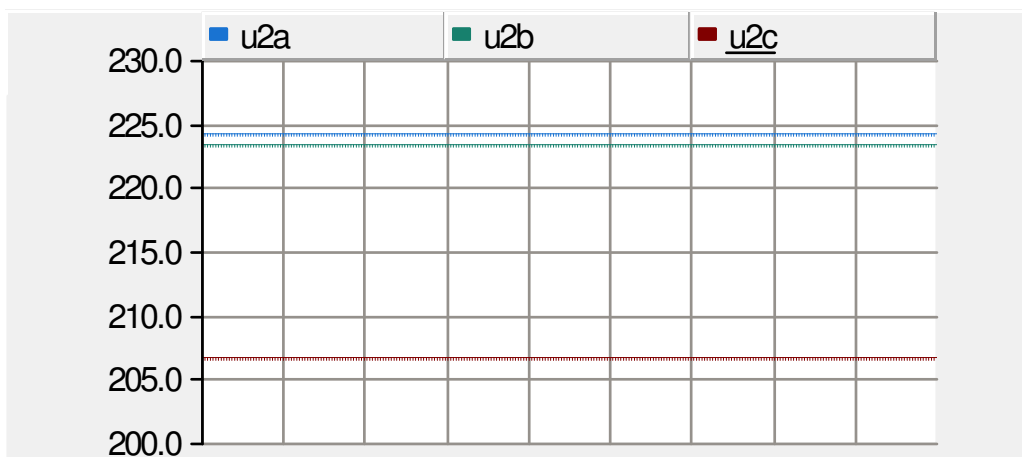


Figure 4.4. 50 Hz components of phase voltages (V) at the end of the line

Voltage in phase with the single-phase load is 206.6 V. this means about a 10% difference from the 230 V nominal value. The unbalanced load also causes a rise in the neutral RMS voltage. This is presented in Figure 4.5.

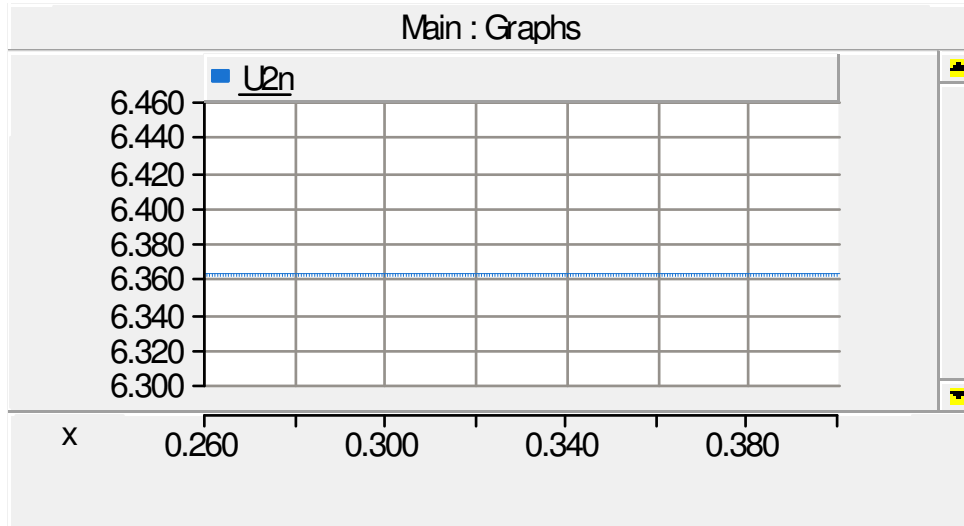


Figure 4.5. RMS neutral-to-ground voltage (V) at the end of the line

The RMS value of neutral-to-ground voltage is 6.36 V RMS. This means peak-to-peak variation in neutral is about 18 V ($2 \cdot 6.36 \cdot \sqrt{2} = 18.0$ V).

4.2.2 Hybrid system with symmetric AC load

In this case, the symmetric AC load is the same 90 kW, but now the 10 kW additional load is connected to a DC bus instead of to the AC phase. Figure 4.6 displays phase voltages at the end of the line, while Figure 4.7 displays RMS voltage rise in neutral.

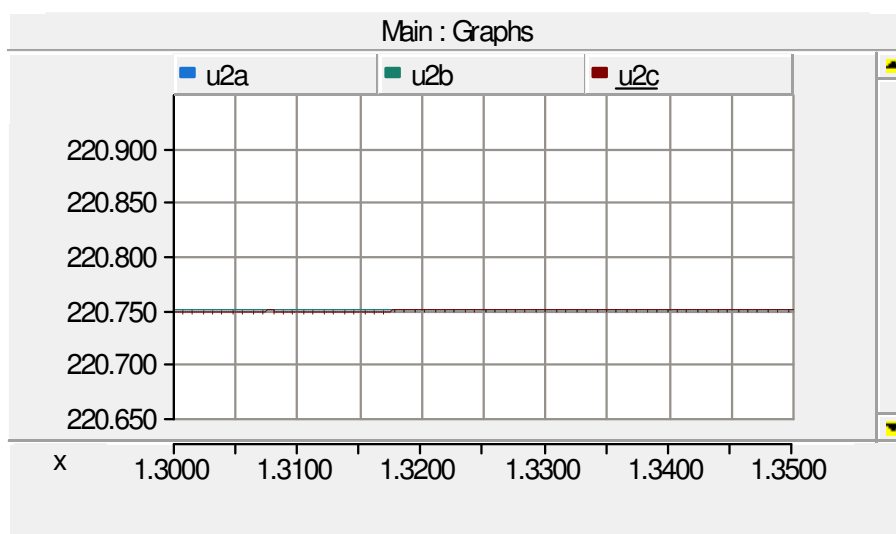


Figure 4.6. 50 Hz components of phase voltages (V) at the end of the line

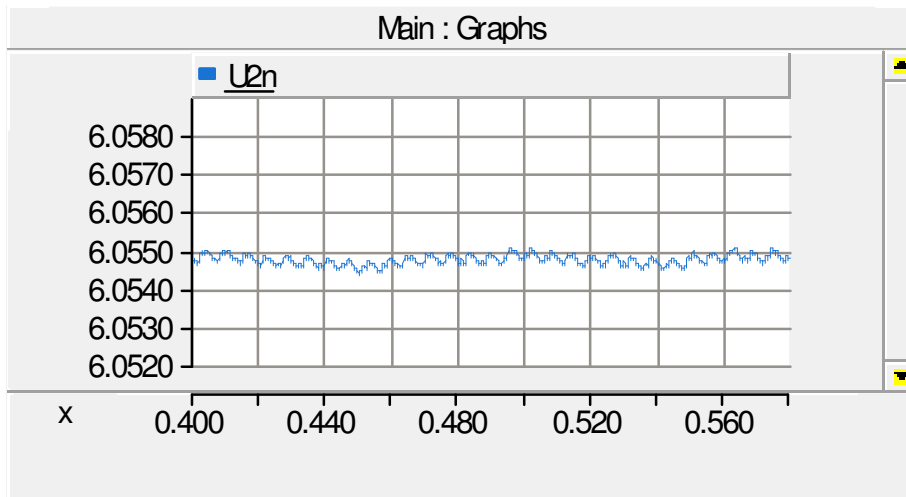


Figure 4.7 RMS neutral-to-ground voltage (V) at the end of the line

Comparing the two results, asymmetric AC load creates large differences between phase voltages, and also a slightly higher rise in neutral-to-ground voltage compared to the hybrid system. The SFS-EN 50160 standard states that line and line-to-line voltages must for 95% of the time be between $\pm 10\%$ of nominal and always within $+10\%$ and -15% for normal power quality. This would mean that when voltage drops due to asymmetric AC load, half of the voltage drop would be caused by the neutral conductor, assuming equal line and neutral conductors. The next simulation therefore targets a 5% voltage drop in the neutral conductor due to DC current as the maximum DC power allowed in the hybrid system.

4.2.3 Hybrid system with 5% voltage rise in neutral

In this case, the AC system has a 90 kW symmetric star-connected load. DC load is adjusted until there is a 5% (11.5 V) voltage rise in neutral-to-ground to find out the maximum DC power value when neutral voltage is the limiter. Figure 4.8 displays a neutral-to-ground voltage rise of 11.5 V, while Figure 4.9 displays the DC power at this voltage rise limit.

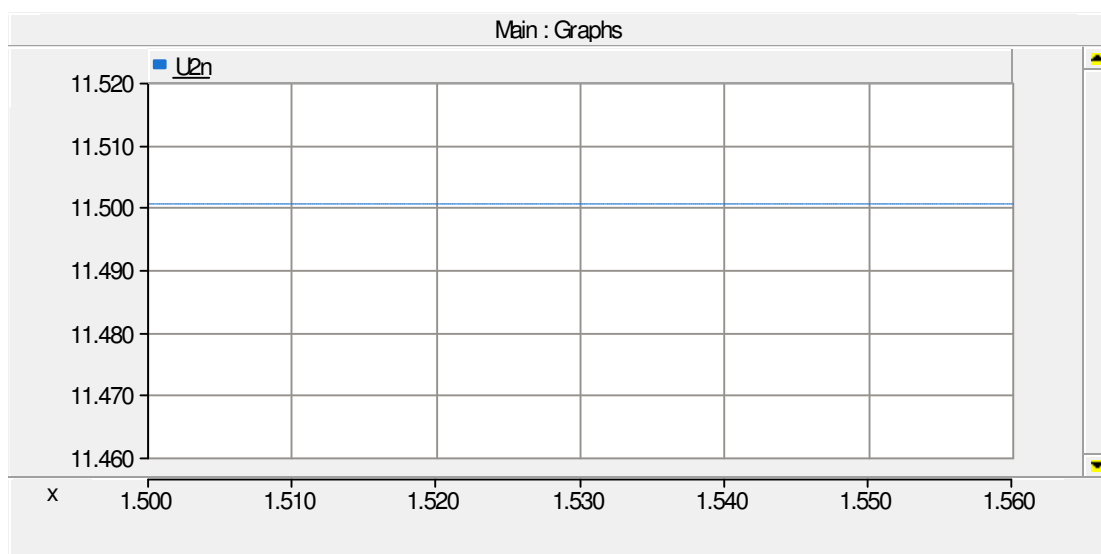


Figure 4.8. Neutral-to-ground voltage (V) at end of the line

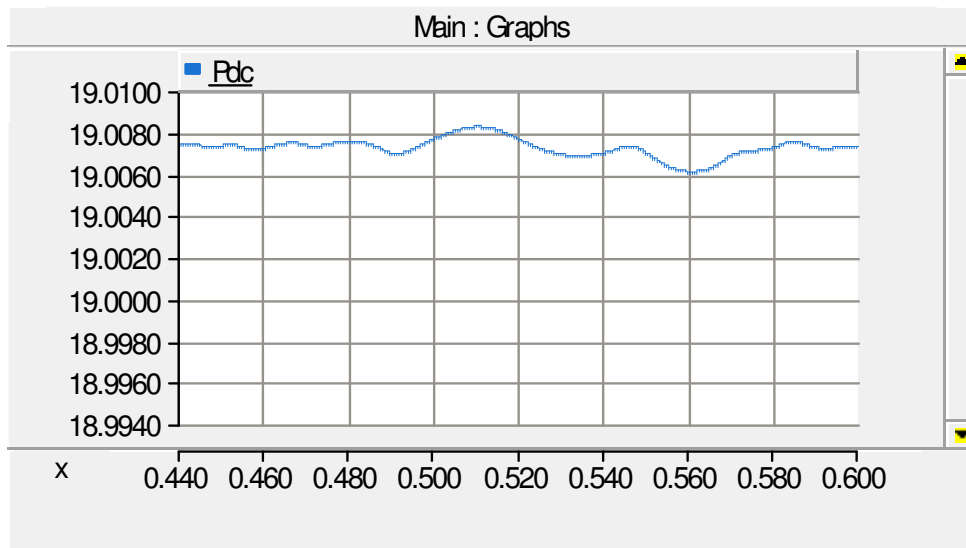


Figure 4.9. DC load power (kW)

The DC system allows 9 kW more power compared to a case where there is 90 kW of symmetric load and 10 kW of single-phase load. Interestingly, if there is a symmetric load of 150 kW on the AC side, the neutral line can take 21.3 kW of DC current at 11.5 V RMS limit, which is more than with the 90 kW AC load. The reason for this is that the DC and AC systems are connected from the star point. With the delta AC load there is not this kind of effect.

4.2.4 Hybrid system with AC unbalance

In this simulation base, the setup is the same as in the first simulation: 90 kW symmetric star-connected load and 10 kW single-phase load (at c-phase). In addition to these, the maximum amount of DC load is used until neutral-to-ground voltage rises to 11.5 V (RMS). Figure 4.10 displays the DC power measured from simulation using 50 Hz RMS measurement (green) and by multiplying current and voltage (blue).

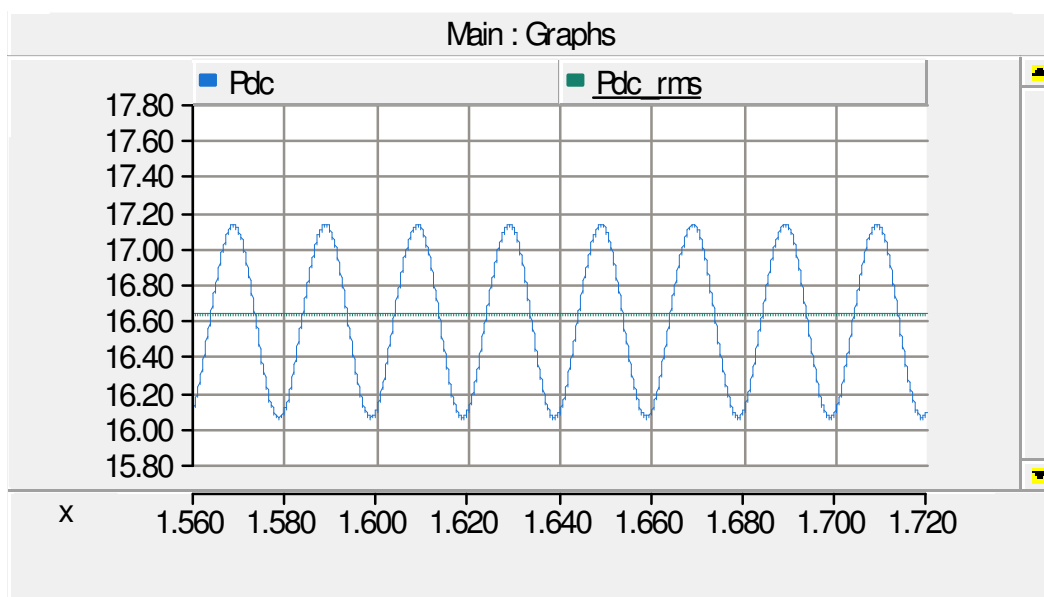


Figure 4.10. DC load power kW. Blue is calculated by multiplying current and voltage and green measured with a 50 Hz RMS meter.

The difference in the power curves results from the fact that the AC system is creating a 50 Hz fluctuation in neutral-to-ground voltage. Figure 4.11 displays this fluctuation in DC voltage.

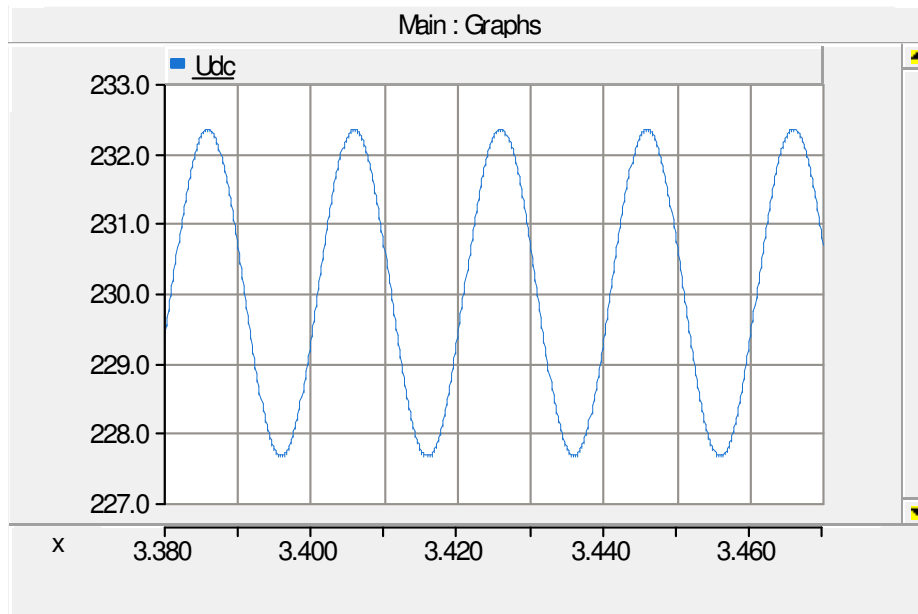


Figure 4.11. 50 Hz fluctuation in DC voltage (V)

Voltage fluctuation in the DC line is minimal in the figure and would cause no problems with DC loads.

4.3 DC voltage adjusted to the peak value of AC voltage

The DC voltage level and the peak value of AC voltage are considered comparable in terms of electrical safety and also when classifying the low voltage limit as 1000 VAC or 1500 VDC ($\sqrt{2} \cdot 1000V = 1414 V$). [9] From this point of view, DC voltage could be 325 V in this kind of hybrid concept if there is a standard 230 V in the AC system. Of course, the LV definition allows much higher voltages, but the voltage level must also be compatible with devices. Should the DC voltage level be too high for most devices, we could use medium DC voltage instead if there is in any case a need for more conversions. In theory, most power electronic single-phase AC devices can also be used with DC voltage when the voltage level is 156 V–325 V, with 156 V being the peak value of the 110V LV system and 325 V the same value for the 230 V LV system. Nowadays most devices have universal power supplies capable of operating with 50 Hz and 60 Hz systems, and therefore with both voltage levels. DC voltage would simply pass the rectifier section of the single-phase AC device. There can be problems with some active rectifiers, however.

4.3.1 Hybrid system, 90 kW symmetric AC, 5% voltage rise in neutral

In this case, the AC system has a 90 kW symmetric star-connected load. DC load is adjusted until there is a 5% (11.5 V) voltage rise in neutral-to-ground to establish the maximum DC power value when neutral voltage is the limiter. The result is 23.2 kW of DC using a 325 V DC voltage level. Figure 4.12 displays measured DC power.

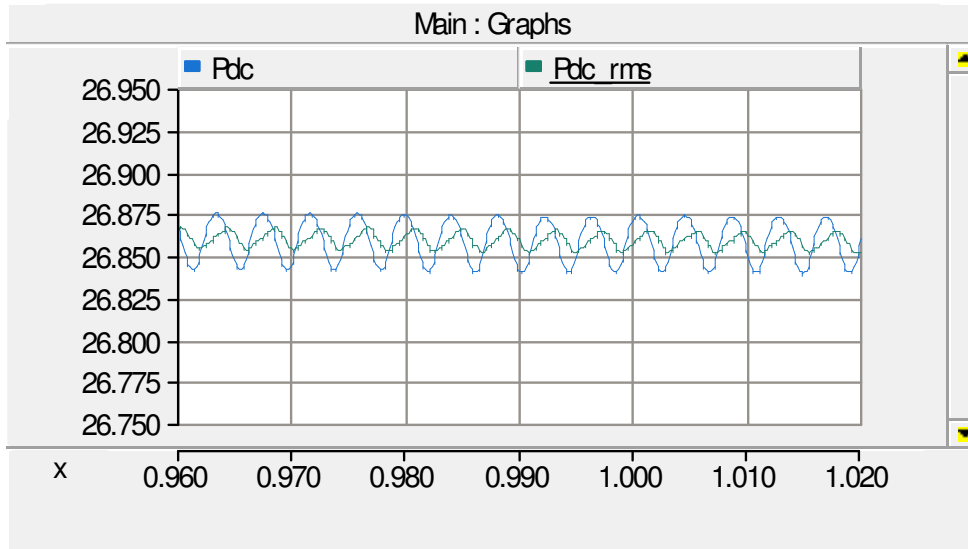


Figure 4.12. Measured DC power at an 11.5 V neutral-to-ground RMS limit

The DC power limit in this case is about 26.85 kW. This result could be predicted by comparing results with 230 V DC and taking account of a 41.3% increase in voltage, which means current can be raised 41.3% for the same voltage drop. ($19 \text{ kW} * 1.413 = 26.847 \text{ kW}$) As with 230 V voltage, DC power can be also increased when symmetric AC power is increased to 150 kW. DC power limit in this case is 30 kW.

4.3.2 Hybrid system, 90 kW symmetric +10 kW single-phase AC, 5% voltage rise in neutral

Here the case is the same as the previous one, but now there is 10 kW additional single-phase load.

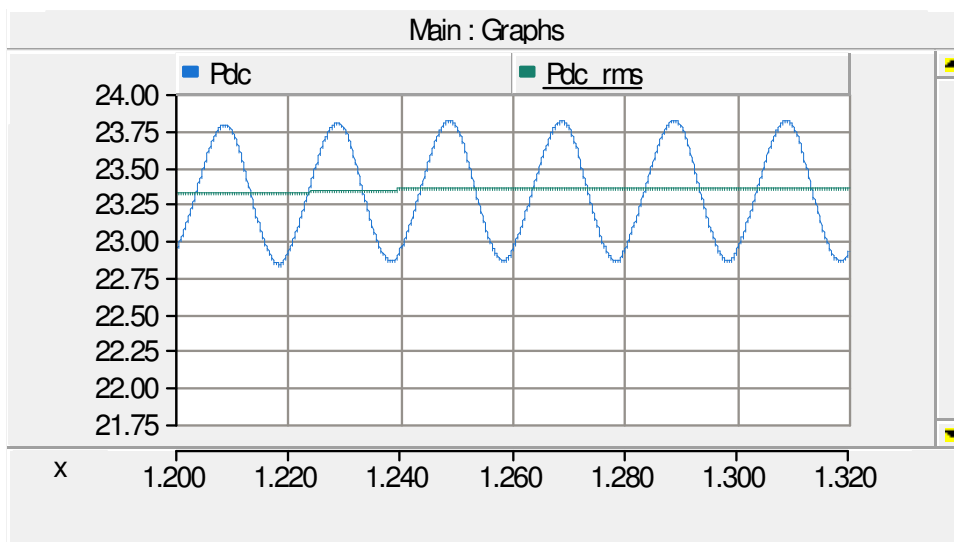


Figure 4.13. DC power (kW) when neutral has risen to 11.5 V RMS

Adding the 10 kW single-phase load decreased DC capacity by 3.6 kW, from 26.85 kW to 23.25 kW.

4.3.3 Hybrid system maximum power with 325 V DC voltage

Here the total hybrid system capacity is tested when DC voltage is 325 V and AC load 90 kW symmetric and 10 kW single-phase. This capacity is found by adjusting AC load power to a point where the voltage drop is 10% on phase voltage, and by adjusting DC power until the RMS voltage rise in neutral-to-ground voltage is 11.5 V. Figure 4.14 displays the neutral-to-ground RMS voltage.

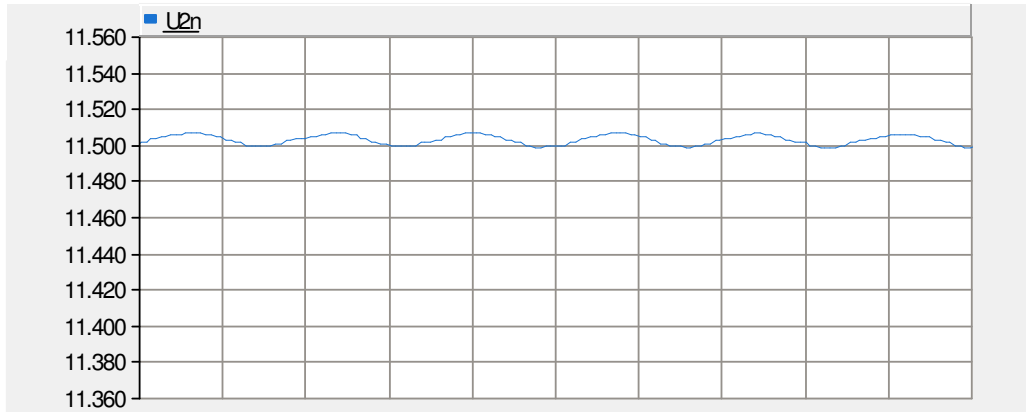


Figure 4.14. Neutral-to-ground RMS voltage (V)

Neutral-to-ground voltage has a fluctuation which results from fluctuating DC voltage. The DC/DC converter output varies and creates fluctuation in the DC load, modelled with a resistor. Figure 4.15 displays the DC load power.

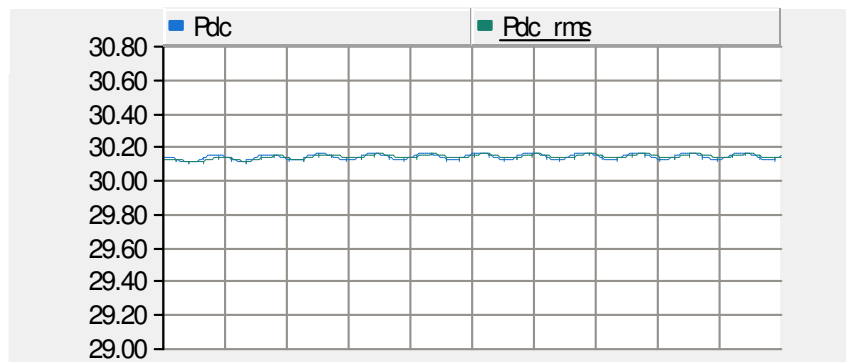


Figure 4.15. DC system power when neutral has risen to 11.5 V RMS (kW)

The same variation mentioned previously also appears in load power measurement.

4.4 Fault simulations

4.4.1 Overcurrent protection for the AC part of the concept

Overcurrent protection protects system devices and conductors from continuous power overloads over nominal power capacity which could cause damage to the system or to individuals. Short-circuit faults cause much higher currents, and voltage supply to these faults must be removed much more rapidly.

According to the SFS-6000-4-43 standard [10], thermal limits in seconds can be calculated by:

Equation 7

$$\sqrt{t} = k \times \frac{S}{I}$$

Where, t = maximum time in seconds, S = cross-cut area of conductor in mm^2 , k -factor dependent on wire type, and I = RMS value of current. According to SFS-6000-4-43, factor k for Al 185 with PVC insulation is 76. [10]

Maximum short-circuit current is achieved when there is a three-phase short circuit in the strongest part of the system. In this case it is behind the isolation transformer, when the inverter is assumed to be connected straight to the transformer and a fault between the two would be considered. Figure 4.16 displays RMS currents in short circuit in this locations.

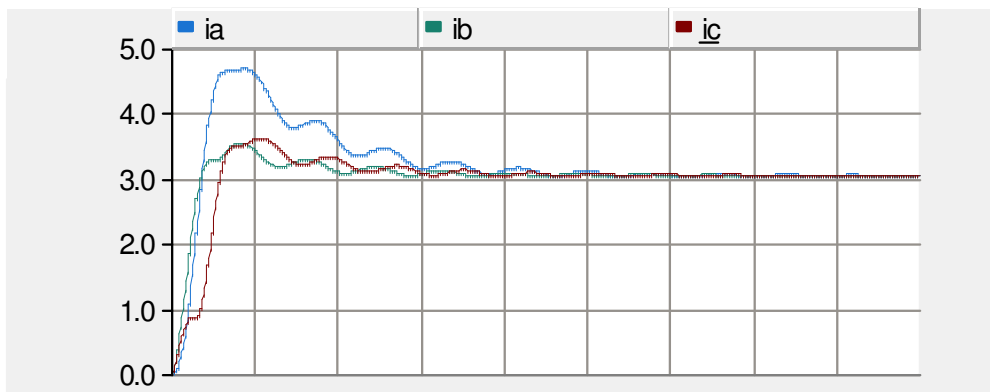


Figure 4.16. RMS short-circuit currents (kA) in three-phase fault at point after transformer

The peak value of the RMS fault current is 4.7 kA in the figure. By calculating t from Equation 7 we get 8.95 s. Although this is quite easy to achieve even with fuse protection, overcurrent relay protection is needed because the system is also designed to allow it to be fed from the inverter. Maximum AC power for symmetric load was 150 kW from the previous simulations, equating to 216.5 A of current. From the point of view of inverter protection, the inverter controls the maximum current allowed internally. Due to capacity constraint, the inverter cannot output high short-circuit current for a long period. In a study and test carried out by NREL [11], the maximum short-circuit current was 2 to 3 times the nominal peak value, while duration times were from 1.1 ms to 4.25 ms. The peak value of the current in a system with nominal power of 150 kW is 306 A. With the multiplier 3 (indicated by [11]), this would mean a maximum short-circuit current peak value of 919 A.

Overcurrent protection simulation

An OC relay with two triggering rules is used, the low setting of 210 A and 2 s and high setting of 215 A and 20 ms being the settings for tripping. The first test is performed without protection to see how much the preliminary inverter model built to PSCAD can output. The test is the same as in Figure 4.16, except that now the current is supplied by the inverter and not by an external grid connection.

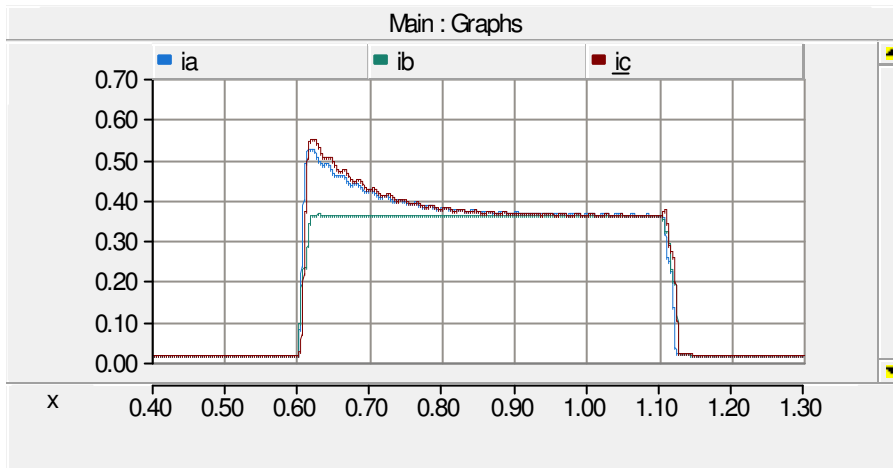


Figure 4.17. Short-circuit current (kA) RMS value supplied by the inverter

The internal control logic here is set to limit current components I_D and I_Q individually to 300 A. It can be seen in the figure that this limiting does not work very well, as the current peaks at the start. The peak value in the fault is 1.8 times the nominal current. An internal limiter for total output current (instead of components) is added to the simulation in Figure 4.18.

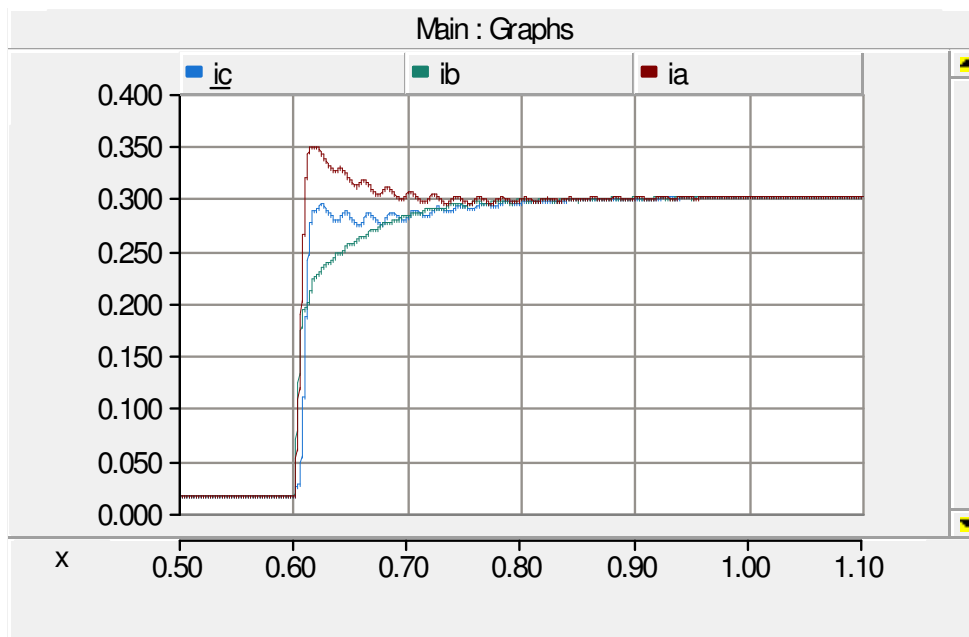


Figure 4.18. Internal limiter added to the inverter to limit total current to 0.3 kA RMS value

The RMS value of the current is limited internally to 300 A. This new type of internal limiter is in use in the remaining simulations. Using this limiter and the relay settings mentioned, protection can open the circuit breaker in 100 ms. This is presented in Figure 4.19.

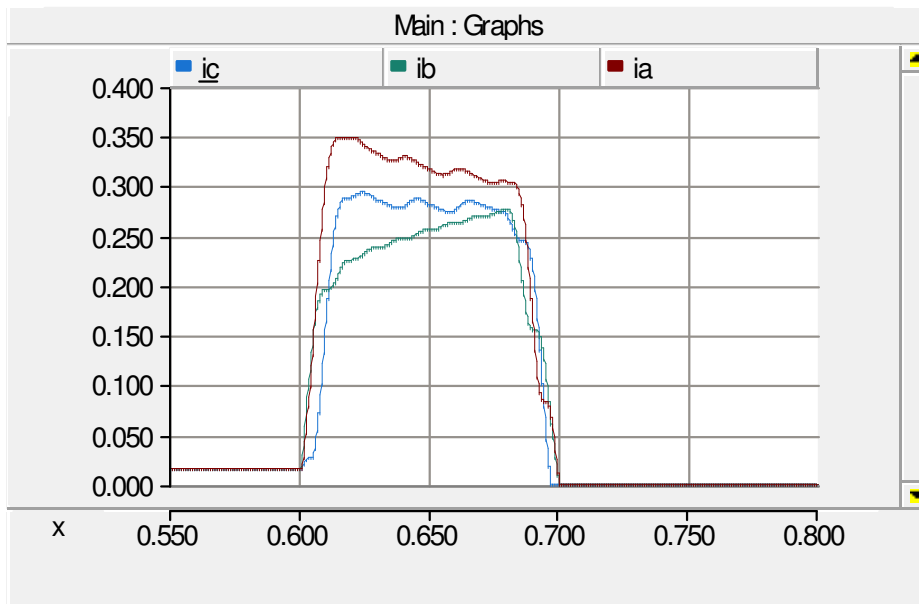


Figure 4.19. Current during a fault where the circuit breaker takes 100 ms to operate. Fault current (kA)

Operation time would naturally be shorter if there was higher load before the fault. If the fault is located at the end of the line there is the following fault curve, presented in Figure 4.20.

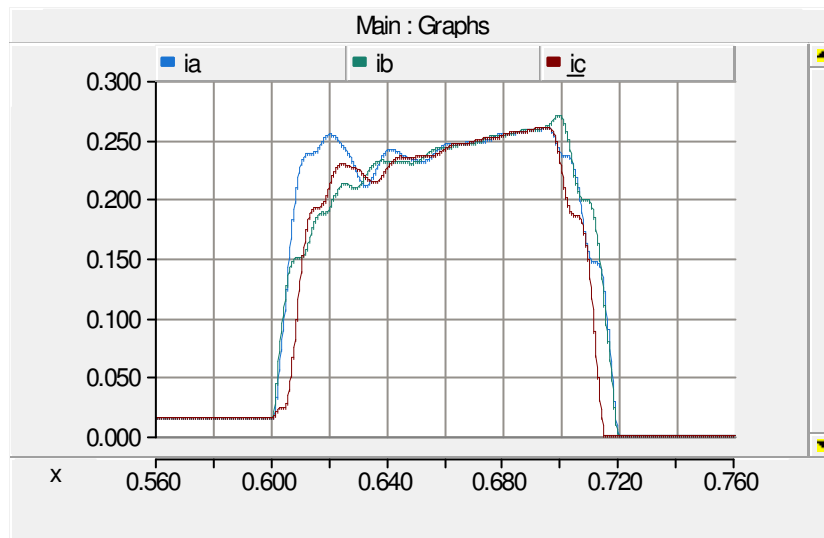


Figure 4.20. Three-phase fault current at the end of the line in the model (kA)

Although the fault current is lower, the fault still is registered in the relay's range of high setting.

4.4.2 Overcurrent protection for the DC system

As the PSCAD main library and project-related library lack comprehensive models for DC circuit breakers and relays, the DC overcurrent protection studies here are conducted solely by inspecting voltage and currents with different faults. An ideal circuit breaker could, of course, be used, but this would not really give any meaningful information. A model of a DC protection relay would therefore be a good thing to have in the future. The main difficulty in breaking DC current vs. AC current is that where current changes polarity there is no point at which opening of the breaker can be achieved without much effort. This means that as there is current flowing in at the time of the circuit breaker operation, an electrical arc will form

forces in the contact gap that will try to prevent it from opening. Figure 4.21 displays the short-circuit current of the DC system when 0.01 ohm resistance is inserted to model the fault between the lines.

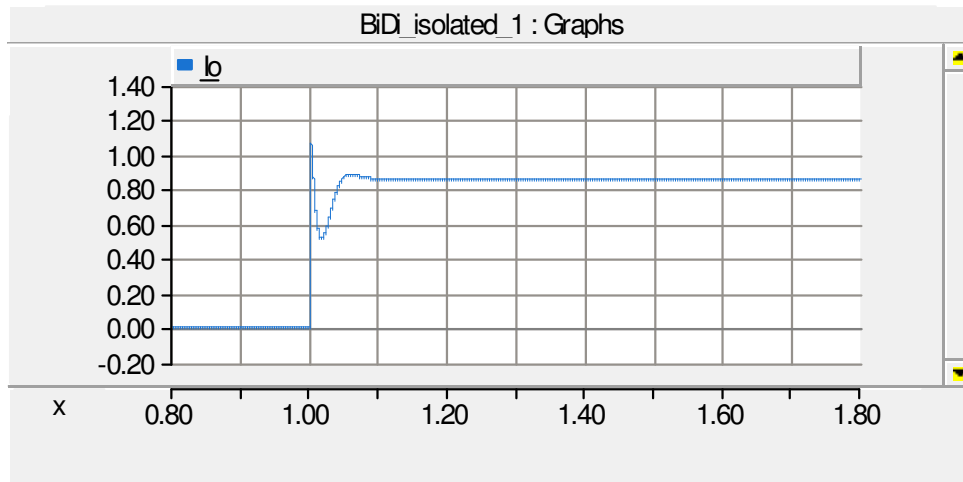


Figure 4.21. Short-circuit current on the DC side without internal current limiting (kA)

No internal current limiting is enabled in the simulation presented in Figure 4.21. Realistically, there is always an internal current limiting device. Figure 4.22 displays the short-circuit current when the DC/DC converter has internal current limiting set to 100 A.

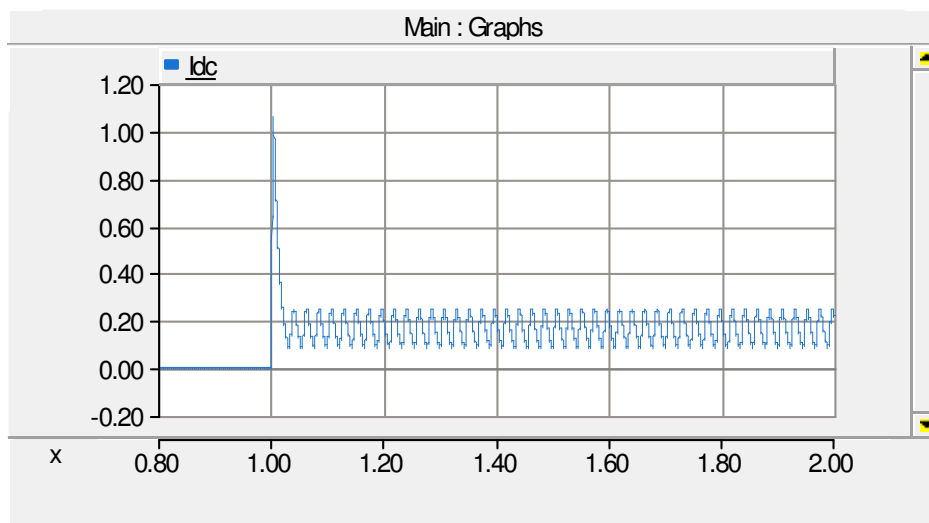


Figure 4.22. Short-circuit current in the DC system with internal current limited to 0.1 kA

The peak value of the current is still the same because the limiter is simply a programmed limiter. In this way it is impossible to prevent the spike when low resistance is inserted into the line with a normal voltage level.

4.4.3 Overvoltage protection

According to the SFS-6000 standard, overvoltage protection is required in places in Finland where there are 25 or more days with thunder. Overvoltage caused by disconnection of generators and loads is usually lower and therefore covered by the protection for

atmospheric-derived overvoltage. Overvoltage resilience requirements for 50 Hz overvoltage for devices in a low voltage system are as follows:

$$U_0 + 250 \text{ V}, t > 5 \text{ s}$$

$$U_0 + 1200 \text{ V}, t < 5 \text{ s}$$

For impulse-type faults (lightning, etc.) resilience requirements vary depending on the overvoltage resilience class (1 to 4). Table 2 displays these as presented in the SFS-6000 standard (in Finnish).

Table 2. Impulse voltage resilience requirements for different equipment classifications

Asennuksen nimellisjännite ^a V	Laitteille vaadittu impulssiylijännitteen kestävyys kV ^b			
	Laitteet asennuksen liittymiskohdassa (ylijänniteluokka IV)	Pää- ja ryhmäjohtojen laitteet (ylijänniteluokka III)	Laitteet (ylijänniteluokka II)	Erityisesti suojatut laitteet (ylijänniteluokka I)
230/400	6	4	2,5	1,5
400/690	8	6	4	2,5
1000	12	8	6	4

^a SFS-EN 60038 mukaan

^b Tämä jännite johdetaan äärijohtimien ja suojajohdinpiirin välille.

Overvoltage protection is required for generators, however. The EN 50438 standard which applies to units under 50 kVA in Finland states that protection acts in 0.2 s when voltage is over 10% or under 15% of nominal. The DC system in this concept falls into this category with a maximum power of 21.3 kW with 230 V voltage and 30 kW with 325 V. The maximum capacity of the AC system in the concept is 150 kW, which means protection for which the settings would have to be configured case by case according to recommendations from Finnish Energy Industries [12].

4.4.4 Combined neutral conductor fault simulations

The combined neutral and DC conductor is the main component of the concept, and therefore critical for operation. In this chapter, neutral faults are simulated to see the kind of problems that arise. In the test, the AC side is loaded with 90 kW symmetrically and with 10 kW single-phase load. The DC-side load is 16.6 kW. Conditions are therefore the same as in 4.2.4.

Combined neutral conductor breaks from grounding point

Figure 4.23 displays the DC-side voltages when the combined neutral conductor is disconnected from the grounding point at the AC distribution transformer at 1.0 s of simulation time.

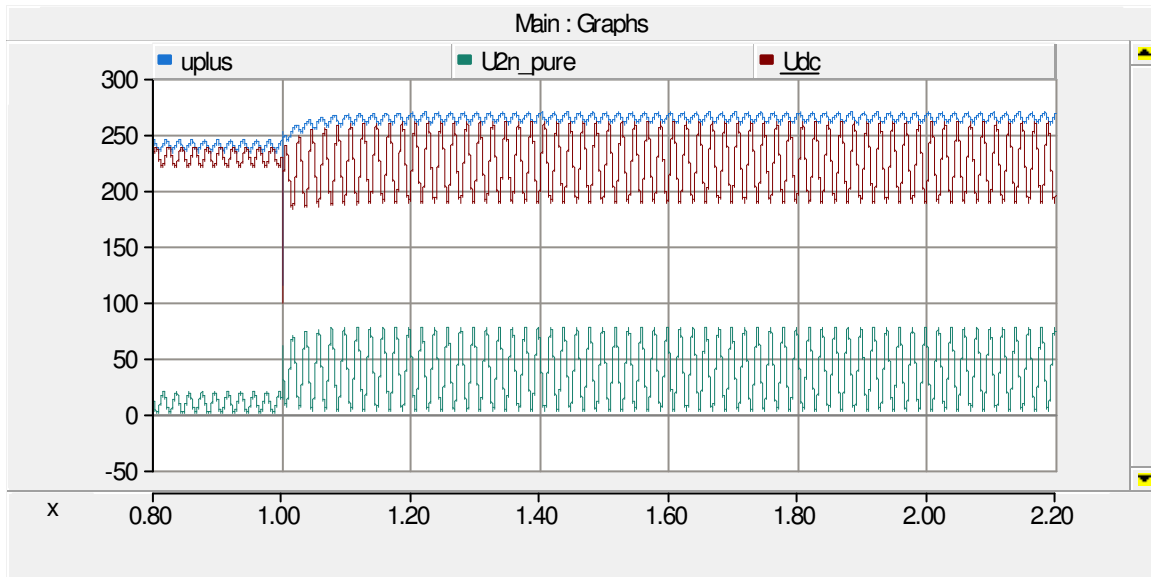


Figure 4.23. DC voltage, DC plus in respect of ground, and combined neutral voltage in respect of ground [V]

Due to the asymmetric AC load, disconnecting of grounding will make neutral-to-ground voltage fluctuate. The DC conductor is now broken and so cannot maintain stable DC voltage across the terminals at the end of the line. The DC current actually now circulates through the secondary side of the transformer, and the DC component is therefore also in line voltages. Base frequency components of AC voltages are presented in Figure 4.24.

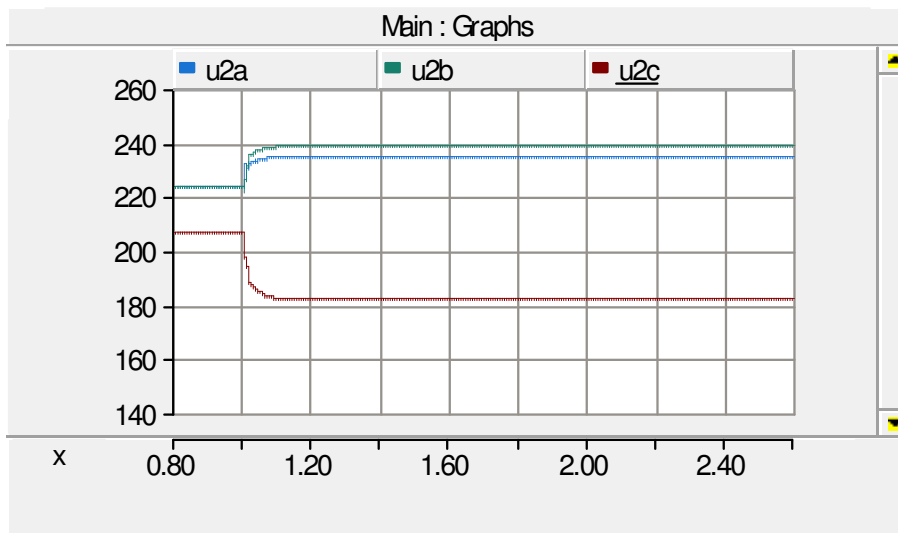


Figure 4.24. RMS base frequency components of AC line voltages

The effect would be much worse if AC in the model was delta type instead of wye (star). Figure 4.25 displays the DC-side voltage when the AC load is delta type.

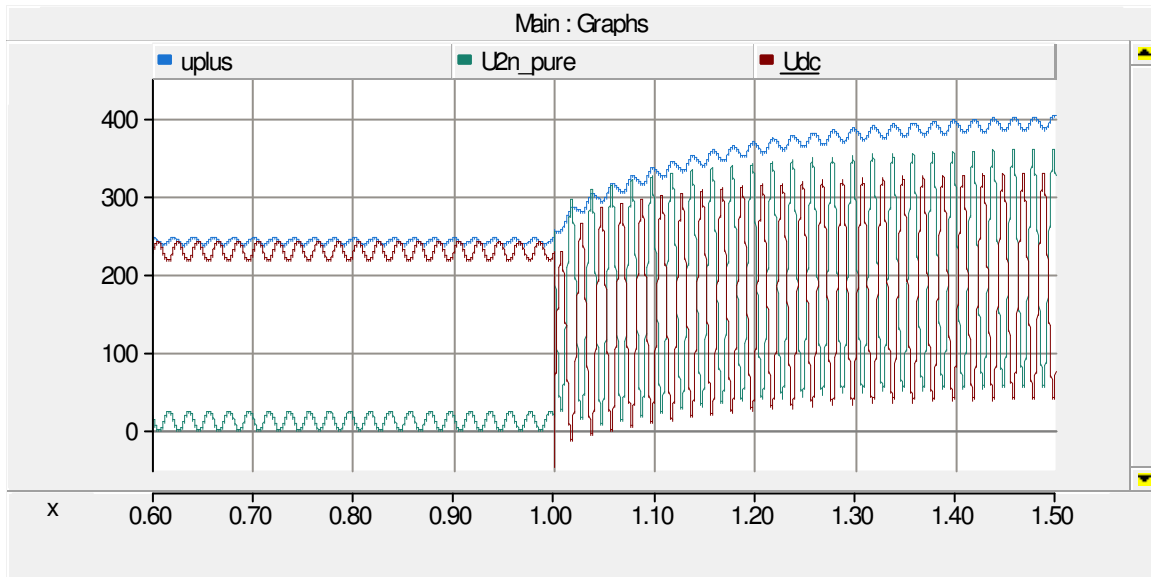


Figure 4.25. DC voltage, DC plus with respect to ground, and combined neutral voltage with respect to ground (V), when AC load is delta type.

Here the combined neutral-to-ground voltage rises to line voltage level. This can also be seen from the AC-side RMS voltages displayed in Figure 4.26.

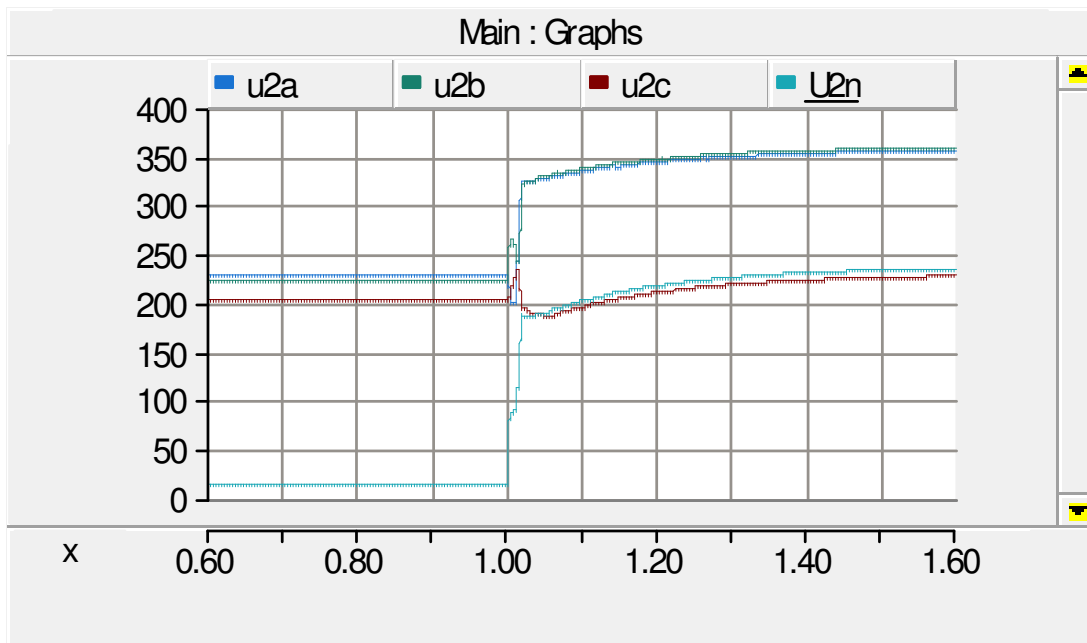


Figure 4.26. RMS voltages at base frequency (V), when the AC load is delta type

All in all, suitable neutral conductor fault detection must be in use. Multiple point grounding would help with the neutral voltage, but this would make fault currents flow in ground loops and this could create hazardous voltages nearby [13]. One tripping rule could be the too-high neutral-to-ground voltage and other presence of the DC component in neutral current (measured from the distribution transformer). Neutral fault detection can also be aided as presented in “Neutral fault management in LV network operation supported by the AMR system” [14].

5. Results

The main focus in the study was on developing a concept and model around the idea of a shared neutral conductor between AC and DC systems. The neutral conductor is unloaded when there is a symmetric three-phase AC load. The idea was to find a use for this capacity by injecting DC current into the neutral line. Focus in the actual simulations was on power capacity, but microgrid operation was also tested successfully. All conductor lines in the study were identical in order to enable identification of the difference between AC and DC capacities. Table 3 displays a summary of the results.

Table 3 Summary of the results of capacity testing

Configuration	AC system	DC system	Total capacity	Limiting factor
AC only	90 kW three phase +10 kW single phase load	-	100 kW	Voltage 10% sag on the line with single phase load
AC+DC (230 V) symmetric	90 kW symmetric	19 kW	109 kW	Neutral RMS voltage 11.5 V
AC+DC (230 V) unbalance	90 kW three phase +10 kW single phase load	16.6 kW	116.6 kW	Neutral RMS voltage 11.5 V
AC + DC (230 V) max power	150 kW three phase load	21.3 kW	171.3 kW	Voltage 10% sag on the line voltages and Neutral RMS voltage 11.5 V
AC+DC (325 V) symmetric	90 kW symmetric	26.9 kW	116.9 kW	Neutral RMS voltage 11.5 V
AC+DC (325 V) unbalance	90 kW three phase +10 kW single phase load	23.3 kW	123.3 kW	Neutral RMS voltage 11.5 V
AC+DC (325 V) max power	150 kW symmetric	30.1 kW	180.1 kW	Voltage 10% sag and Neutral RMS voltage 11.5 V

Simulations were performed with 230 V and 325 V DC voltages. The results indicate that from the total system perspective it is more favourable for this hybrid concept to have DC load than asymmetric AC load. By moving single-phase load to the DC side of the hybrid system, load could be increased from 10 kW to 19 kW (230 V DC simulation). Without removing the single-phase load, DC power could be 16.6 kW at the same time. The DC system also responded well to increased symmetric load of the AC system. DC load power could be increased 12% when symmetric AC load was increased 67% from 90 kW to 150 kW. The reason for this was the star-connected AC load model, and with delta-connected AC load there was no change in DC capacity. Increased voltage level also increased DC power capacity linearly, as can be expected from the DC power equation.

Fault simulations were also carried out in the study concerning three-phase short circuit, short circuit in the DC system, and combined neutral breaking. Relay protection must be used instead of fuses as the overcurrent capacity of the inverter is very limited. Programmable limiting of the fault current was investigated on both the inverter side and the DC side. Programmable limiting of the RMS fault current was more effective in reducing

short-circuit current spike with the AC system than with the DC system. In both cases, limiting of steady overcurrent was very effective. Faults in the combined neutral and DC conductor were also simulated with delta- and wye-connected AC loads. In both cases, power quality was seriously affected due to asymmetric loading in the AC system. Delta-connected load resulted in much worse power quality and voltage fluctuations compared to wye-connected load. The fault was located at the distribution transformer, and thus DC could continue to operate. Power quality was seriously affected with wye AC load, however, as grounding of the neutral was lost (a separate PE conductor was assumed to be functional for device protection). With delta AC load, AC voltage with the DC component was actually introduced into the combined neutral conductor, and the power quality would therefore not be acceptable. For these reasons, effective neutral fault detection is mandatory for the concept.

6. Conclusions

This study examined a hybrid AC/DC distribution concept. Simulations were carried out to establish the technological feasibility of the concept and the performance with regard to power capacities and fault scenarios. It can be concluded from the simulations that it is technologically possible to combine with an AC distribution system using a joint neutral and DC conductor. Power capacity increase by this method is, however, very limited, and varies according to the asymmetric load on the AC side. Increase in symmetric AC load actually increased capacity on DC system opposed to how asymmetric load affected the system. As this study has been carried out from a purely technological perspective, an economic analysis of possible scenarios would be needed to establish the competitiveness of the concept. Because capacity increases are quite modest, they cannot justify the use of this kind of concept. A potential use case in mind is the increased reliability of a parallel DC system providing backup power. The DC system could also be the point where critical loads, such as computers and lighting are connected, and also a simpler way of connecting small-scale generation. The use of DC sockets would be a simple way of differentiating system loads which will be operational when the AC grid is down.

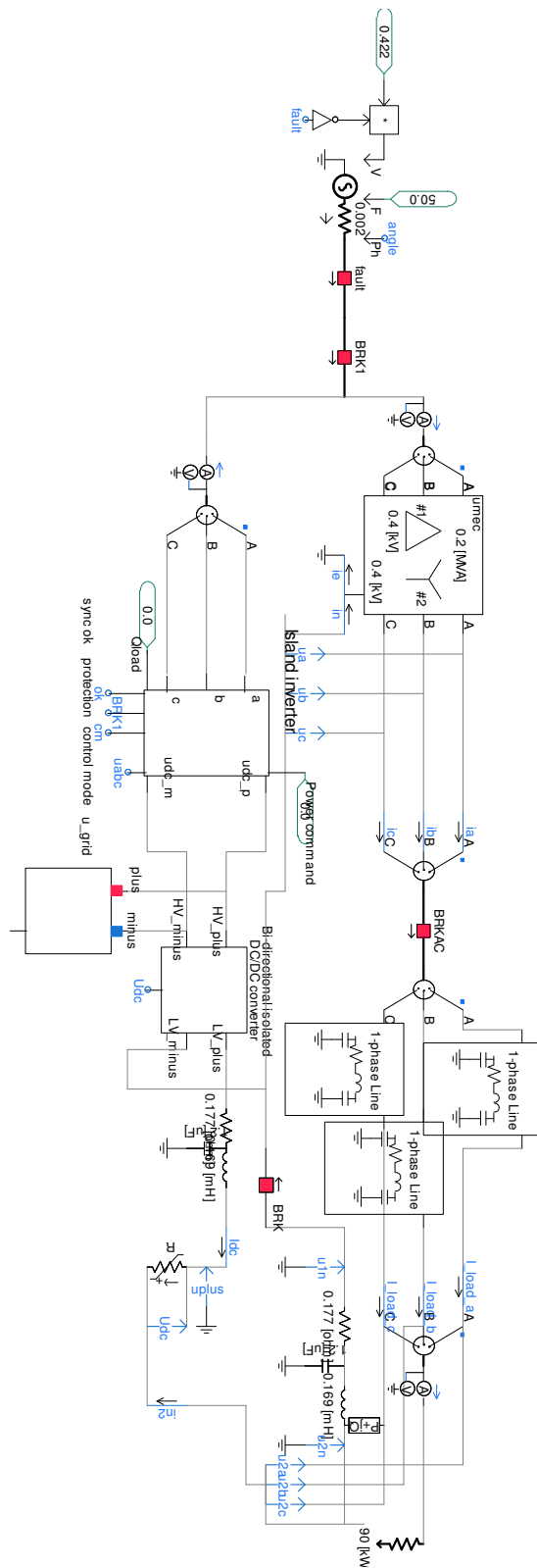
From the reliability and safety perspective, LVDC is a good option, but one that should be built truly independently from the AC system, with no shared wire and “weak point”. In Germany, small-scale generation can be as much as the nominal transformer capacity, but in practice the limit is close to 70% due to voltage fluctuations on higher penetrations [15]. It is clear that the hybrid concept as presented cannot accept the same amount of renewable capacity if all of it is connected to a DC bus. However, the DC system could play a part in solving the problem by balancing the variations with the DC bus, load control in DC loads, and Var control at the inverter.

References

- [1] Pasonen, R. Model of Bi-directional Flyback Converter for Hybrid AC/DC Distribution. International Journal of Power Electronics and Drive Systems, Vol. 3, No. 4, December 2013, pp. 444~449.
- [2] Sizing and Protection of the Neutral Conductor. Electrical engineering portal EEP. Available at : <http://electrical-engineering-portal.com/sizing-and-protection-of-the-neutral-conductor-1>
- [3] Pasonen, R. Energy centre microgrid model. VTT Technical Research Centre of Finland. 2011. VTT Working Papers 182. 34 p. <http://www.vtt.fi/inf/pdf/workingpapers/2011/W182.pdf>

- [4] Green, T., Prodanovic, M. "Control of inverter-based micro-grids" Electric Power Systems Research, Volume 77, Issue 9, Distributed Generation, July 2007.
- [5] Luomi, J. Sähkökoneiden muutosilmiöt 816 B. Otakustantamo. 1982.
- [6] Gergaud, O., Rogib, G., Multon, B., Ben Ahmed, H. Energy modelling of a lead-acid battery within hybrid wind/photovoltaic systems. 2003. ENS Cachan, Bruz, France.
- [7] Peng, F. Z. Photovoltaic Module Model based on the Manufacturer Data Sheet. Michigan State University. Available at:
<http://www.egr.msu.edu/pelab/projects/project%20pdf%20files/PV%20Module%20Model.pdf>
- [8] Reka cable values. Available at: <http://www.reka.fi/eng/products/814>
- [9] Low voltage directive overview explained. Available at: <https://cemarking.net/low-voltage-directive/>
- [10] SFS 6000-4-43 Low-voltage electrical installations. Part 4-43: Protection for safety. Protection against overcurrent. SESKO ry, electrotechnical standardization association of Finland.
- [11] Keller, J., Kroposki, B. Understanding Fault Characteristics of Inverter - Based Distributed Energy Resources. NREL technical report. 2010. Available at:
<http://www.nrel.gov/docs/fy10osti/46698.pdf>
- [12] Lehto, I. Technical appendix 2 Technical requirements concerning generation installations of over 50 kVA. Finnish Energy Industries. 2011. Available at:
<http://energia.fi/sahkomarkkinat/sahkoverkko/pientuotanto>
- [13] Zipse, D., W., The Hazardous multigrounded neutral distribution system and dangerous stray currents. Petroleum and Chemical Industry Conference 2003. West Chester, USA .23 p. Available at:
<http://ieeexplore.ieee.org/stamp/stamp.jsp?arnumber=1242596>
- [14] Mäkinen A, and others. Neutral fault management in LV network operation supported by AMR system. Cired 22 nd International Conference on Electricity Distribution. Stockholm, 10-13 June 2013. Available at:
http://www.cired.net/publications/cired2013/pdfs/CIRE2013_1214_final.pdf
- [15] Impact of photovoltaic generation on power quality in urban areas with high PV population. 2008 Germany. Available at
http://www.pvupscale.org/IMG/pdf/WP4_D4-3_public_v1c.pdf

Appendix A: Representation of model in PSCAD



Appendix B: Control logic of inverter in grid connected mode

